

**EUR 4408 e**

EUROPEAN ATOMIC ENERGY COMMUNITY - EURATOM

**SORA DYNAMICS AND CONTROL SYSTEM  
STUDIES USING MEAN-VALUE  
NEUTRON KINETICS EQUATIONS**

by

**R. ARHAN**

**1970**



**Joint Nuclear Research Center  
Ispra Establishment - Italy**

**Reactor Physics Department  
Research Reactors**

## LEGAL NOTICE

This document was prepared under the sponsorship of the Commission of the European Communities.

Neither the Commission of the European Communities, its contractors nor any person acting on their behalf :

make any warranty or representation, express or implied, with respect to the accuracy, completeness or usefulness of the information contained in this document, or that the use of any information, apparatus, method or process disclosed in this document may not infringe privately owned rights; or

assume any liability with respect to the use of, or for damages resulting from the use of any information, apparatus, method or process disclosed in this document.

This report is on sale at the addresses listed on cover page 4

at the price of FF 13.80	FB 125.—	DM 9.20	Lit. 1 560	Fl. 9.—
--------------------------	----------	---------	------------	---------

**When ordering, please quote the EUR number and the title, which are indicated on the cover of each report.**

Printed by Guyot, s.a.  
Brussels, January 1970

This document was reproduced on the basis of the best available copy.

**EUR 4408 e**

EUROPEAN ATOMIC ENERGY COMMUNITY - EURATOM

SORA DYNAMICS AND CONTROL SYSTEM  
STUDIES USING MEAN-VALUE  
NEUTRON KINETICS EQUATIONS

by

R. ARHAN

1970



Joint Nuclear Research Center  
Ispra Establishment - Italy

Reactor Physics Department  
Research Reactors

## **ABSTRACT**

The study described in this report deals with dynamics and control of the pulsed fast reactor SORA. It is based on a set of equations for mean-value neutron kinetics. A simulation of the complete set of equations, including thermal reactivity feed-back, is performed. As results, the reactor responses to perturbations of reactivity, inlet coolant temperature and coolant velocity are shown. Control rod malfunctions are investigated; a start-up procedure is proposed. A fast control system is synthesized.

---

## **KEYWORDS**

SORA	COOLANTS
REACTIVITY	TEMPERATURE
NEUTRONS	VELOCITY
KINETIC EQUATIONS	CONTROL ELEMENTS
DISTURBANCES	STARTUP

TABLE OF CONTENTS

- 1. Introduction
- 2. Basic Equations for Description of the Reactor
  - 2.1 Core kinetics - Conversion to power
  - 2.2 Reactor thermal description
  - 2.3 Reactivity feedback
  - 2.4 Summary of equations
- 3. Simulation of the Uncontrolled Reactor
- 4. Startup Procedure
- 5. Linearized Reactor Description
- 6. Fast Control System
  - 6.1 Closing the loop directly
  - 6.2 First improvement of the fast control system performances
  - 6.3 Second improvement of the fast control system performances
  - 6.4 Basic set of equations for the controlled reactor
- 7. Malfunctions
- 8. Conclusion
  
- Appendix 1 - Derivation of numerical values for a steady state condition at power
- Appendix 2 - Derivation of numerical values for subcritical steady state condition
- Appendix 3 - Reactor period.
  
- Nomenclature
- Note on the simulation
- Literature

-----



SORA DYNAMICS AND CONTROL SYSTEM STUDIES USING MEAN-VALUE  
NEUTRON KINETICS EQUATIONS\*)

---

I. INTRODUCTION

The SORA reactor is a fast reactor periodically pulsed by reactivity variations designed as a neutron source for research in neutron physics. The reactor design and experimental use have been described in several meetings, notably at Karlsruhe in 1965 (Ref. 6), at Santa Fe in 1967 (Ref. 7) and at Albuquerque in 1969 (Ref. 4).

The study described in the report was performed in the year 1968 at the request of the SORA Project to answer questions which the project designers had about the reactor dynamics and control.

Mean-value neutron kinetics equations are used for this study. A set of equations for the reactor mean temperatures is used for the calculation of thermal reactivity feedback.

A simulation of the complete set of equations is performed using the digital computer IBM 360/65. As results, the reactor responses to perturbations of reactivity, inlet coolant temperature, and coolant velocity are shown. Also a start-up procedure is proposed. Control rod malfunctions occurring in the uncontrolled reactor are also investigated.

In a classical manner, the set of equations is linearized for small deviations from pulsed steady state to obtain a reactor transfer function which is used for the synthesis of the fast control system. This fast control system is then introduced as a control loop around the reactor. The whole system is then simulated and checked against typical perturbations of reactivity, inlet coolant temperature and coolant velocity.

I wish to acknowledge the help and the interesting suggestions of Mr. Larrimore throughout this study.

---

\*) Manuscript received on 10 September 1969.

## 2. Basic Equations for Description of the Reactor

---

A block-diagram for dynamics of the uncontrolled reactor is shown in figure 2. See also the list of symbols at the end of this report. Three parts may be seen in this block diagram:

- core kinetics and conversion to power
- thermal description
- reactivity feedback.

Three inputs are considered for this system:

- external reactivity ( $\epsilon_d$ )
- inlet coolant temperature ( $T_{c,in}$ )
- coolant velocity ( $V_{cool}$ ).

The three most important outputs (from dynamics point of view) are shown:

- power ( $\bar{P}$ )
- fuel temperature ( $\bar{T}_f$ )
- structure temperature ( $\bar{T}_g$ ).

Also available from the set of equations that we will use are a number of other parameters such as fission rate, outlet coolant temperature, internal reactivities from fuel and structure. For reasons of clarity all of these parameters were not shown in Fig. 2.

We will analyze now this block-diagram and present the relative sets of equations.

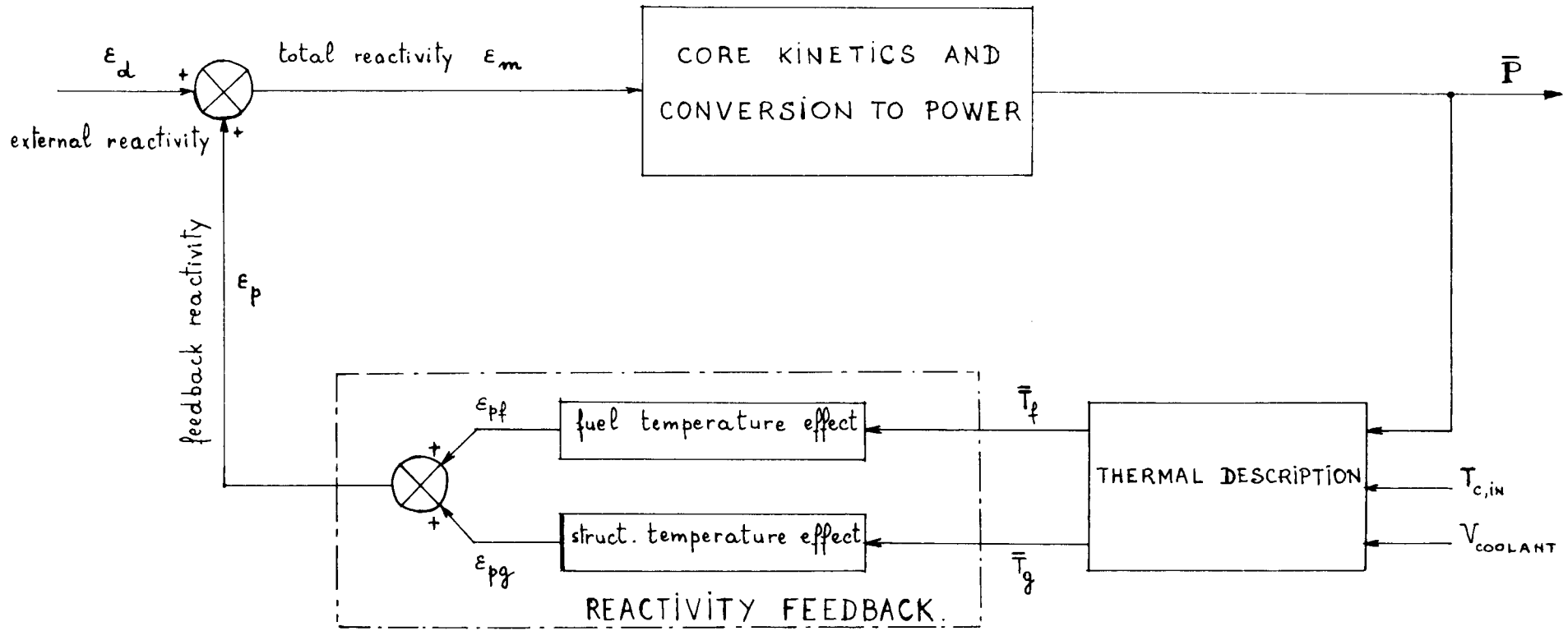


FIG.2. General block-diagram for dynamics of the uncontrolled reactor.

## 2.1 Core kinetics - Conversion to power

The kinetic theory of a periodically pulsed reactor was established by Bondarenko and Staviskii (Ref.1). Later on, extensive kinetic studies were performed at Ispra, namely by Blässer, Misenta and Raievski (Ref.2). The necessary elements for a clear understanding of the present report will be found in the survey paper of Larrimore (Ref. 3).

Since our main purpose was to get a good approximation for the reactor transients and a reference design for control systems, we decided to use "mean power kinetics" in a point reactor model for such a work. By "mean power kinetics" we mean the time behaviour of the average values over a period of the power and precursor concentrations for times long compared to the pulse period.

In analogy with the multiplication factor for a stationary (non pulsed) reactor, a multiplication factor  $K$  is here defined, based (Ref. 2) on production and destruction of delayed neutron precursors:

$$K = \frac{\text{Precursor Production During Period}}{\text{Precursor Decay During Period}} \quad (2-1-1)$$

with  $K = 1$  for pulsed steady-state operation. This multiplication factor, also called "pulsed multiplication coefficient" may be expressed as:

$$K = \frac{M}{T} + \frac{\beta}{\epsilon_0} \quad (2-1-2)$$

where  $M$  and  $\epsilon_0$  are functions of the reactivity level in the reactor. In Figure 2-1 a plot (Ref. 4) of  $K$  versus peak prompt reactivity  $\epsilon_m$ , calculated for the SORA reactor, is shown. The represented curve was fitted as:

$$K = 0,229 + 8,80 \epsilon_m + 0,0176 e^{4140 \epsilon_m} \quad (2-1-3)$$

Now, since the precursor production during a period is  $\beta v \bar{w} T$  and the precursor decay during the same time interval is  $\sum_i \lambda_i \bar{c}_i T$  it results directly from (2-1-1) that the mean fission rate is:

$$\bar{w} = \frac{K}{\beta v} (\sum_i \lambda_i \bar{c}_i + s_0) \quad (2-1-4)$$

while the mean delayed neutron precursor concentrations are described by:

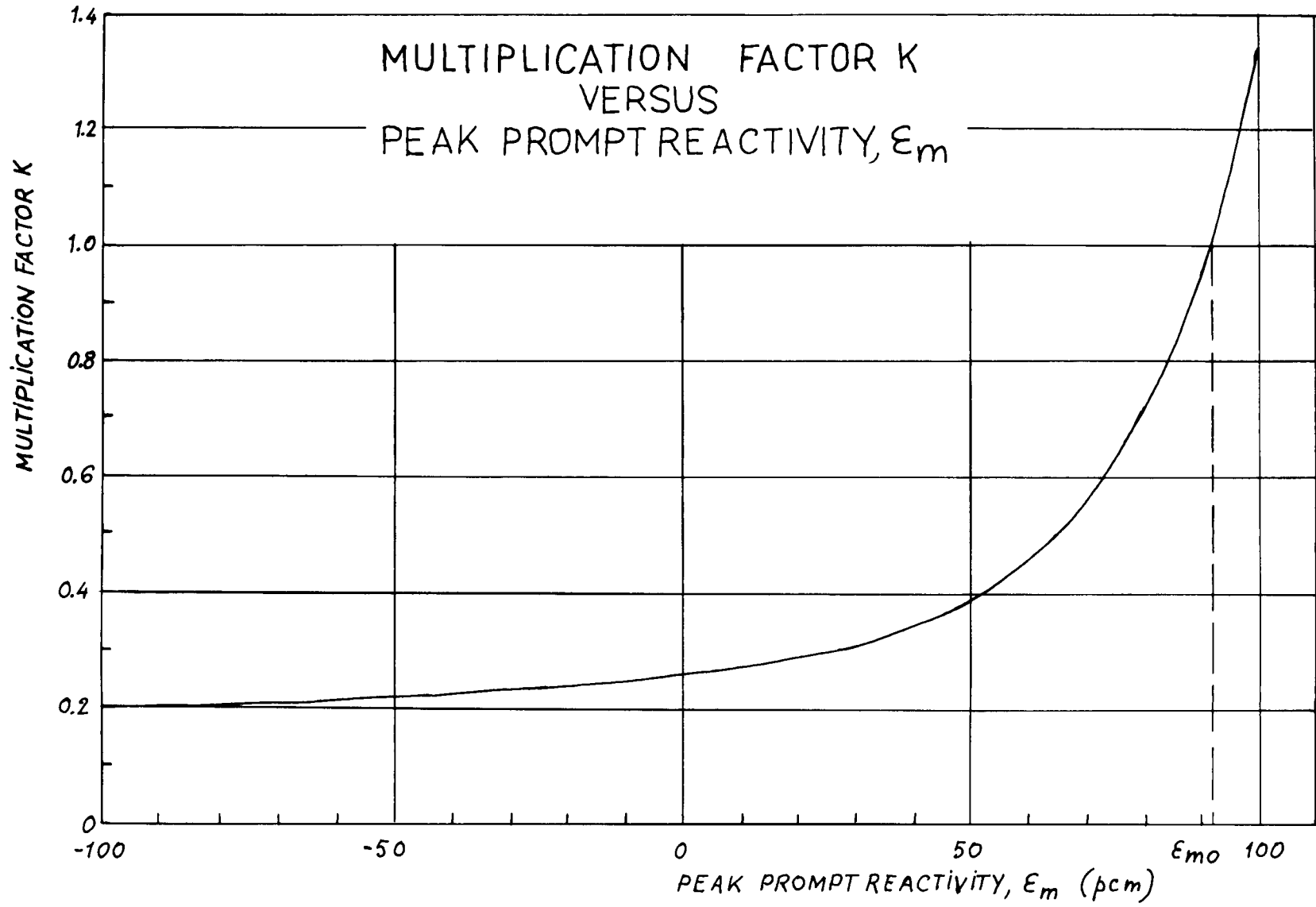


FIG. 2.1

$$\frac{d\bar{C}_i}{dt} = \beta_i v \bar{w} - \lambda_i \bar{C}_i. \quad (2-1-5)$$

Equations (2-1-2) to (2-1-5) describe completely the reactor kinetics. The corresponding reactor power is straight forwardly obtainable from the mean fission rate  $\bar{w}$  as:

$$\bar{P} = \frac{\bar{w}}{C_f} \quad (2-1-6).$$

We will write finally the complete and practical set of equations for kinetics:

$$\begin{aligned} K &= 0,229 + 8,80 \epsilon_m + 0,0176 e^{4140 \epsilon_m} \\ \bar{w} &= \frac{K}{\beta v} (\sum_i \lambda_i \bar{C}_i + S_0) \\ \frac{d\bar{C}_i}{dt} &= \beta_i v \bar{w} - \lambda_i \bar{C}_i \\ \bar{P} &= \frac{\bar{w}}{C_f} \end{aligned} \quad (2-1)$$

## 2.2 Reactor thermal description

A simple mathematical model (Ref. 5) for the reactor thermal description has been developed in collaboration with the SORA Project, which expresses the mean fuel and structure temperatures in terms of the power, the inlet coolant temperature and the coolant velocity. These mean temperatures are used for the calculation of thermal reactivity feedback.

The SORA reactor core consists of a bundle of approximately 116 fuel rods (Ref. 6 and 7). Assuming a uniform radial power generation and neglecting the heat flow in the vertical direction, a temperature distribution such as shown in Fig. 2-2 may be defined for any element, which enables us to calculate mean temperatures for fuel, bond-clad, and coolant. The heat exchange coefficients, calculated from these mean temperatures, are assumed to hold in in transients around the previous steady state.

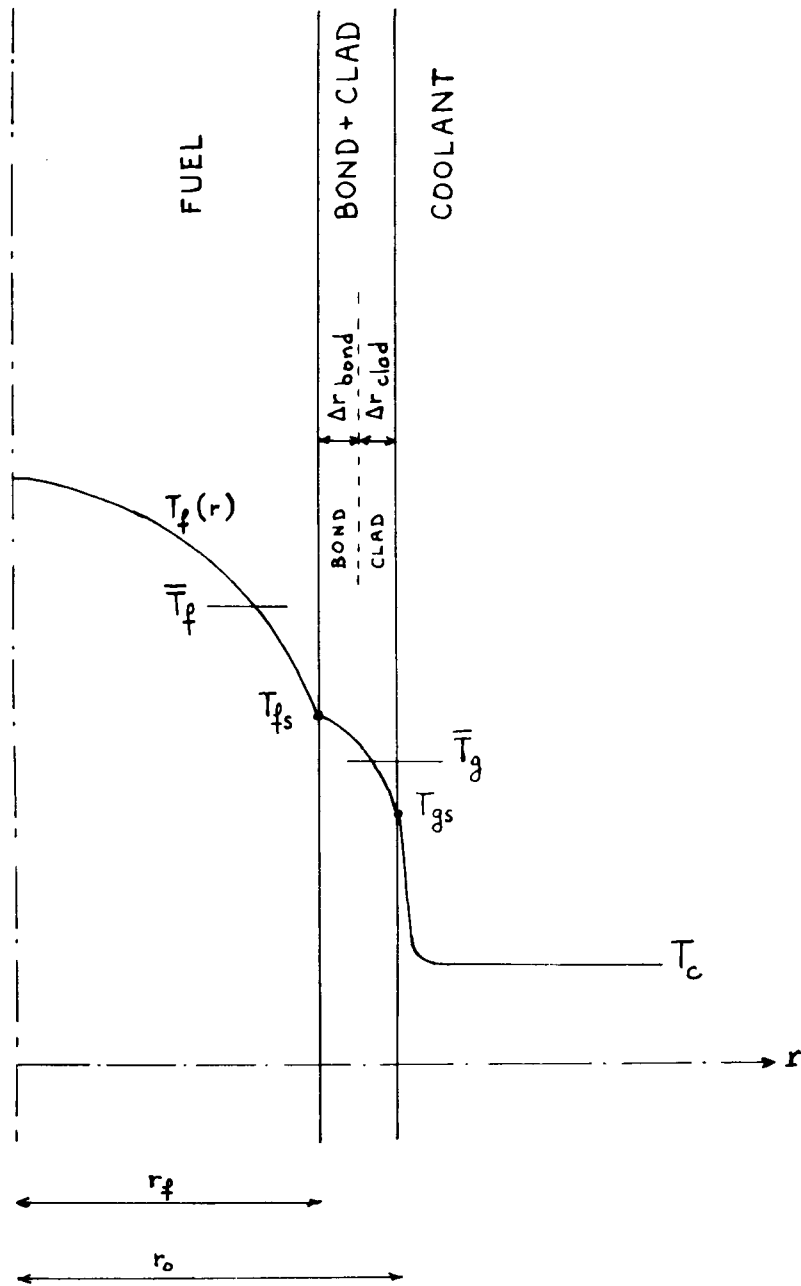


Figure 2.2 . Temperature distribution.

2-2-1. Steady-state temperature distributions. Mean temperatures (see figure 2-2).

2-2-1-1. Temperature distribution in fuel. Mean fuel temperature  $\bar{T}_f$ .

Assuming a uniform volume heat source  $q''$ , and  $k_f$  independent of the temperature, the temperature distribution in a fuel element is a solution of:

$$q'' + k_f \nabla^2 T_f = 0.$$

Neglecting heat flow in the axial direction, this may be written as:

$$\frac{1}{r} \cdot \frac{d}{dr} \left( r \frac{dT_f}{dr} \right) = - \frac{q''}{k_f}.$$

Integrating once:

$$\int_0^r d \left( \frac{rdT_f}{dr} \right) = - \frac{q''}{k_f} \int_0^r r dr \quad \left( \frac{dT_f}{dr} = 0 \text{ at } r = 0 \right)$$

$$\frac{dT_f}{dr} = - \frac{q''}{2k_f} r$$

Integrating again:

$$\int_{T_f(r)}^{T_{fs}} dT_f = - \frac{q''}{2k_f} \int_r^{r_f} r dr$$

$$T_f(r) - T_{fs} = - \frac{q''}{4k_f} r_f^2 \left[ 1 - \left( \frac{r}{r_f} \right)^2 \right].$$

The mean fuel temperature is defined as:

$$\bar{T}_f - T_{fs} = \frac{\int_0^{r_f} \left[ T_f(r) - T_{fs} \right] 2\pi r dr}{\int_0^{r_f} 2\pi r dr}$$

$$\bar{T}_f - T_{fs} = \frac{q''}{8k_f} r_f^2 .$$

Introducing finally the average power generation in fuel per unit of length  $q = \pi r_f^2 q''$  , we obtain:

$$\bar{T}_f = \frac{q}{8\pi k_f} + T_{fs} .$$

2-2-1-2. Temperature distribution in bond-clad. Mean structure temperature  $\bar{T}_g$ .

For the purpose of this study the bond and clad are combined into a single region. Due to the small thickness, one may write directly (see figure 2-2):

$$T_{fs} - T_{gs} = \frac{q''}{k_g} (r_o - r_f)$$

where  $q''$  is the average power per unit area. Introducing the average power generation per unit of length  $q = 2\pi r_f q''$  , we get:

$$T_{fs} - T_{gs} = \frac{q}{2\pi r_f k_g} (r_o - r_f)$$

The mean bond-clad or structure temperature is then defined as:

$$\bar{T}_g = T_{gs} + \frac{1}{2} (T_{fs} - T_{gs}) = T_{gs} + \frac{q}{4\pi k_g} \left( \frac{r_o - r_f}{r_f} \right)$$

or:

$$\bar{T}_g = T_{fs} - \frac{1}{2} (T_{fs} - T_{gs}) = T_{fs} - \frac{q}{4\pi k_g} \left( \frac{r_o - r_f}{r_f} \right).$$

2-2-1-3. Temperature distribution in the coolant. Mean coolant temperature (or coolant temperature at half height of core)  $T_c$ .

We assume the coolant temperature increases linearly from the inlet to the outlet so that the mean coolant temperature is the coolant temperature at half height of core. Following this assumption:

$$T_{gs} - T_c = \frac{q''}{h_f}$$

where  $h_f$  is the heat transfer coefficient between clad and coolant and  $q''$  the average power per unit area. Introducing once again the average power generation per unit of length we obtain:

$$T_{gs} - T_c = \frac{q}{2\pi r_f h_f} \cdot$$

### 2-2-2. Steady state heat transfer coefficients

From the previous equations we derive heat exchange coefficients related to the characteristic temperatures  $\bar{T}_f$ ,  $\bar{T}_g$ , and  $T_c$ .

#### 2-2-2-1. Fuel to clad heat transfer coefficient $h_{Fs}$

We have found:

$$\bar{T}_f - T_{fs} = \frac{q}{8\pi k_f}$$

$$T_{fs} - \bar{T}_g = \frac{q}{4\pi k_g} \left( \frac{r_o - r_f}{r_f} \right).$$

Defining the heat transfer coefficient  $h_{Fs}$  as:

$$h_{Fs} = \frac{q}{\bar{T}_f - \bar{T}_g}$$

we obtain:

$$h_{Fs} = \frac{1}{\frac{1}{8\pi k_f} + \frac{1}{4\pi k_g} \left( \frac{r_o - r_f}{r_f} \right)}$$

#### 2-2-2-2. Clad to coolant heat transfer coefficient

$$\bar{T}_g - T_{gs} = \frac{q}{4\pi k_g} \left( \frac{r_o - r_f}{r_f} \right)$$

$$T_{gs} - T_c = \frac{q}{2\pi r_f h_f} \cdot$$

Defining the heat transfer coefficient  $h_{sc}$  as:

$$h_{sc} = \frac{q}{\bar{T}_g - T_c}$$

it is found:

$$h_{sc} = \frac{1}{\frac{1}{4 \pi k_g} \left( \frac{r_o - r_f}{r_f} \right) + \frac{1}{2 \pi r_f h_f}} .$$

### 2-2-3. Heat balance equations

Fuel heat balance equation:

$$C_f \frac{d\bar{T}_f}{dt} = q(t) - h_{FS} (\bar{T}_f - \bar{T}_g) . \quad (2-2-3-1)$$

Bond-clad or structure heat balance equation:

$$C_g \frac{d\bar{T}_g}{dt} = h_{FS} (\bar{T}_f - \bar{T}_g) - h_{sc} (\bar{T}_g - T_c) \quad (2-2-3-2)$$

Coolant heat balance equation:

$$LC_c \frac{dT_c}{dt} = Lh_{sc} (\bar{T}_g - T_c) - VC_c (T_{c,out} - T_{c,in}) \quad (2-2-3-3)$$

$$T_c = \frac{1}{2} (T_{c,in} + T_{c,out}) . \quad (2-2-3-4)$$

Assuming no time lag exists between  $\bar{T}_g$  and  $T_c$  due to the small heat capacity of the coolant, equation (2-2-3-3) may be turned into:

$$Lh_{sc} (\bar{T}_g - T_c) = VC_c (T_{c,out} - T_{c,in}) . \quad (2-2-3-5)$$

Equations (2-2-3-4) and (2-2-3-5) are then used to express  $T_c$  and  $T_{c,out}$  in terms of  $\bar{T}_g$  and  $T_{c,in}$ :

$$T_c = \frac{1}{1 + \frac{Lh_{sc}}{2VC_c}} \cdot \bar{T}_g + \frac{1}{1 + \frac{Lh_{sc}}{2VC_c}} T_{c,in} \quad (2-2-3-6)$$

$$T_{c,out} = \frac{2}{1 + \frac{Lh_{sc}}{2VC_c}} \bar{T}_g - \frac{1 - \frac{2VC_c}{Lh_{sc}}}{1 + \frac{Lh_{sc}}{2VC_c}} T_{c,in} \quad (2-2-3-7)$$

Eliminating finally  $T_c$  between (2-2-3-6) and (2-2-3-2), we get for the structure heat balance equation:

$$C_g \frac{d\bar{T}_g}{dt} = h_{FS} (\bar{T}_f - \bar{T}_g) - \frac{h_{sc}}{1 + \frac{Lh_{sc}}{2VC_c}} (\bar{T}_g - T_{c,in}) \quad (2-2-3-8)$$

#### 2-2-4. Summary of equations for the reactor thermal description

Results (2-2-3-1), (2-2-3-8), (2-2-3-7) and (2-2-3-4) describe the reactor from a thermal point of view. For clarity, we rewrite here these results:

$$\begin{aligned} C_f \frac{d\bar{T}_f}{dt} &= \frac{p}{nL} \cdot \bar{P}(t) - h_{FS} (\bar{T}_f - \bar{T}_g) \\ C_g \frac{d\bar{T}_g}{dt} &= h_{FS} (\bar{T}_f - \bar{T}_g) - \frac{h_{sc}}{1 + \frac{Lh_{sc}}{2VC_c}} (\bar{T}_g - T_{c,in}) \\ T_{c,out} &= T_{c,in} + \frac{2}{1 + \frac{Lh_{sc}}{2VC_c}} (\bar{T}_g - T_{c,in}) \\ T_c &= \frac{1}{2} (T_{c,in} + T_{c,out}) \end{aligned} \quad (2-2)$$

#### 2-3. Reactivity feedback

A fundamental characteristic of the periodically pulsed reactor is that the reactivity is introduced as a "pulse", that is to say introduced rapidly and removed in the same manner. It has been shown (Ref. 8) that the reactivity feedback during the pulse has a negligible effect on the pulse characteristics due to the short duration of the reactivity pulse. However, the reactivity feedback is important when more than one pulse is considered.

The temperature coefficients of reactivity in SORA have been calculated to be negative, which simplifies considerably all problems of control. The temperature effect is split into two parts: the fuel temperature coefficient  $\epsilon_{pf}$  (including fuel axial expansion and Doppler effect) and the structure temperature coefficient  $\epsilon_{pg}$  (including radial structural expansion) so that:

$$\begin{aligned}
 \epsilon_{pf} &= \alpha_f (\bar{T}_f - T_{REF}^*) \\
 \epsilon_{pg} &= \alpha_g (\bar{T}_g - T_{REF}^*) \\
 \epsilon_p &= \epsilon_{pf} + \epsilon_{pg}
 \end{aligned}
 \tag{2-3}$$

with  $\alpha_f$  and  $\alpha_g$  negative.

#### 2-4 Summary of equations

Equations for kinetics, thermal description, and feedback reactivity are rewritten below. (See Fig. 2-4 for the relative block diagram.)

- $\epsilon_d$  = input reactivity signal
- $\epsilon_p$  = total feedback reactivity signal
- $\epsilon_m$  = total reactivity =  $\epsilon_d + \epsilon_p$ .

$$\begin{aligned}
 K &= 0.229 + 8.80 \epsilon_m + 0.0176 e^{4140 \epsilon_m} \\
 \bar{w} &= \frac{K}{\beta v} (\sum_i \lambda_i \bar{C}_i + S_0) \\
 \frac{d\bar{C}_i}{dt} &= \beta v \bar{w} - \lambda_i \bar{C}_i \\
 \bar{P} &= \frac{\bar{w}}{C_F}
 \end{aligned}$$

$$C_f \frac{d\bar{T}_f}{dt} = \rho \bar{P}(t) - h_{FS} (\bar{T}_f - \bar{T}_g)$$

$$C_g \frac{d\bar{T}_g}{dt} = h_{FS} (\bar{T}_f - \bar{T}_g) - \frac{h_{sc}}{1 + \frac{h_{sc}}{2VC_c}} (\bar{T}_g - T_{c,in})$$

$$T_{c,out} = T_{c,in} + \frac{2}{1 + \frac{h_{sc}}{2VC_c}} (\bar{T}_g - T_{c,in})$$

(2-4)

$$T_c = \frac{1}{2} (T_{c,in} + T_{c,out})$$

$$\epsilon_{pf} = \alpha_f (\bar{T}_f - T_{REF}^*)$$

$$\epsilon_{pg} = \alpha_g (\bar{T}_f - T_{REF}^*)$$

$$\epsilon_p = \epsilon_{pf} + \epsilon_{pg}$$

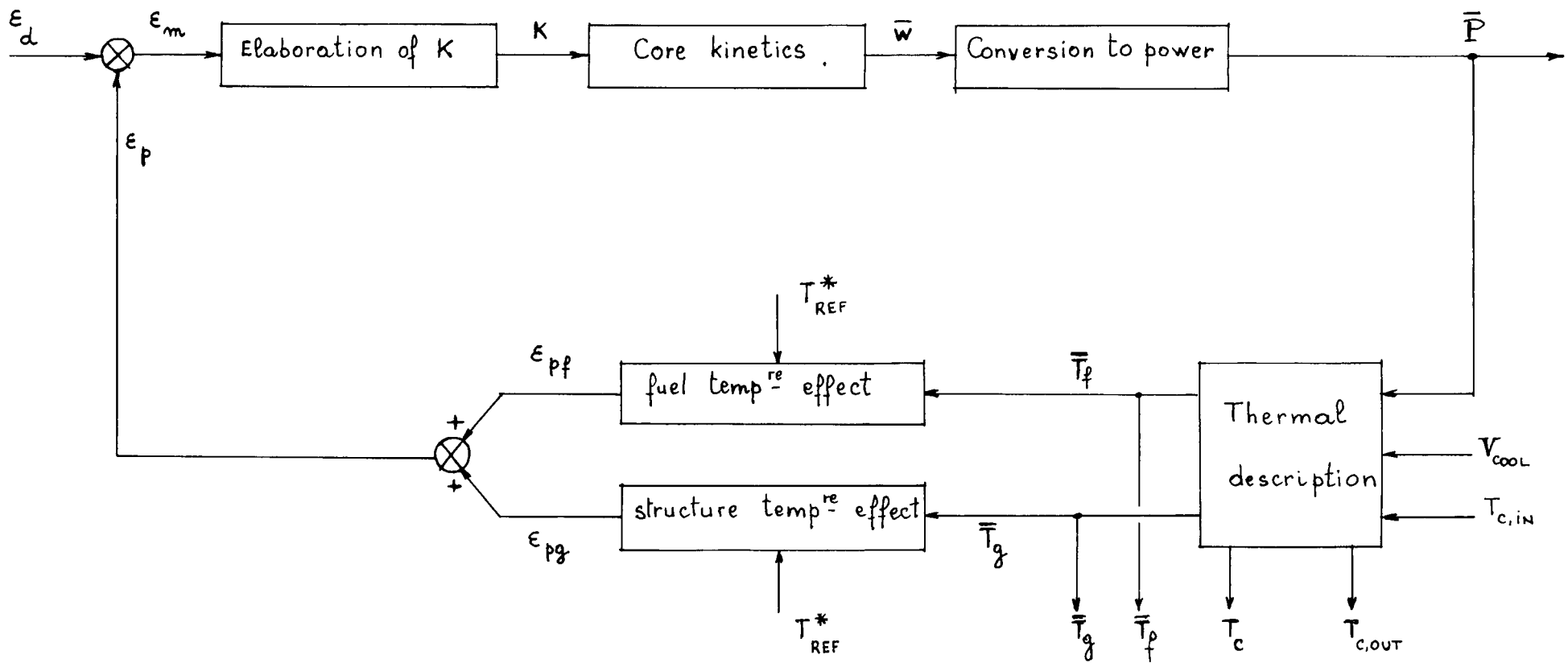


FIG 2.4. BASIC BLOCK-DIAGRAM FOR SORA DYNAMICS.

- see the summary of equations (2.4) -

### 3. Simulation of the Uncontrolled Reactor

The simulation of the uncontrolled reactor was based on the set of equations (2-4). The use of a digital computer rather than an analog one was chosen mainly for the following reasons: noise and thermal drift eliminated, easy calculation of  $K(\epsilon_m)$ , amplitude scale unlimited. Therefore, the simulation consists of an iterative integration of the set of equations (2-4). We used the program SAHYB-2, developed at CETIS: this program was specially developed to meet the requirements of simulation on digital computers (Ref. 9).

It must be noted, however, that an iterative integration by means of a digital computer implies a cumulative error (as time goes on) on the integrated values. But this error may be kept as low as desired by introducing the requested specifications into the program.

We first simulated the effects of:

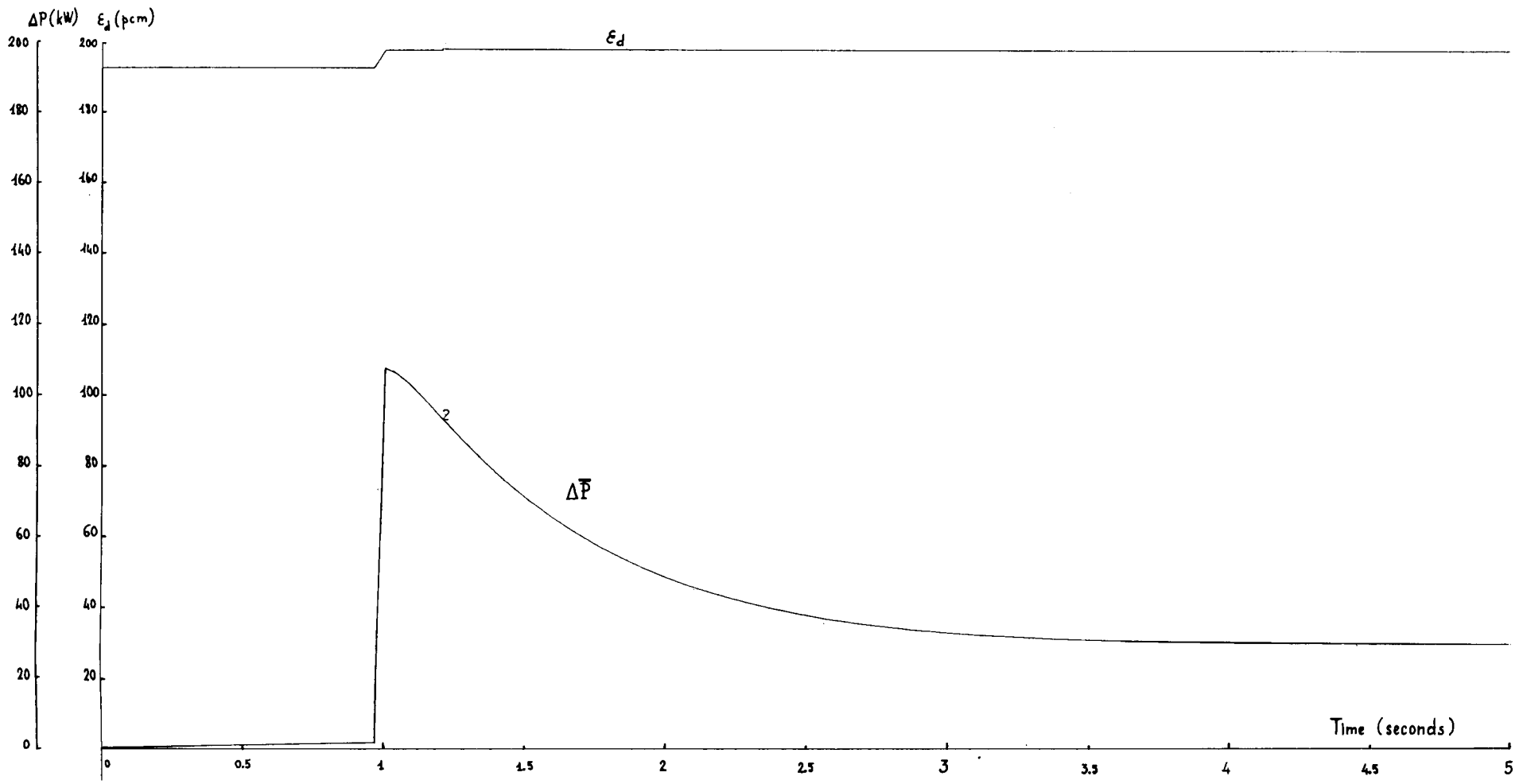
- a change in reactivity,
- a change in coolant velocity, and
- a change in inlet coolant temperature

on the uncontrolled reactor. These changes were introduced as step functions with the reactor assumed to be stabilized at power 600 kW. The relative initial conditions were calculated from the set of equations (2-4) for the steady-state condition\* 600 kW.

In Fig. 3-1 the response to a step of reactivity of 5 pcm is shown: the power jumps immediately by about 100 kW from the initial level 600 kW, which is characteristic of the kinetics of such a reactor (see equation 2-1-4); the power then stabilizes at about 30 kW above the initial level with a time constant of approximately 1 second.

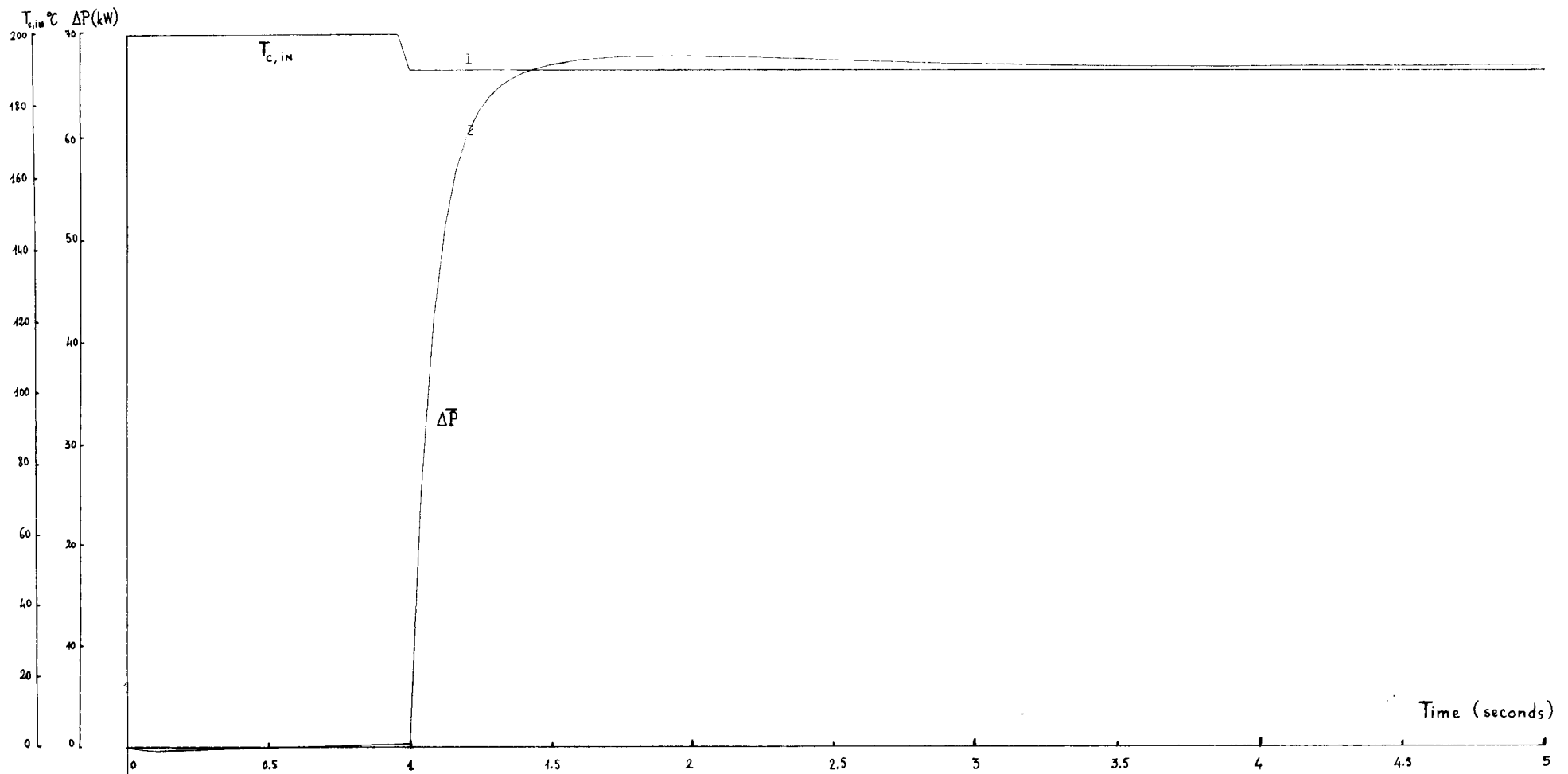
---

\* See the appendix: Derivation of numerical values for a steady-state condition at power.



RESPONSE TO A CHANGE ON REACTIVITY  
 (UNCONTROLLED REACTOR)

FIG. 3-1



RESPONSE TO A CHANGE ON INLET COOLANT TEMPERATURE  
(UNCONTROLLED REACTOR)

FIG. 3-2

In Fig. 3-2, is plotted the power response to a negative step of 10°C on the inlet coolant temperature. The power stabilizes at about 70 kW from the initial level.

Finally, in Fig. 3-3 the power response to a positive step of 0,25 m/s in the coolant velocity is plotted. This results in a power increase of about 10 kW.

In the two last cases, the power level increases due to the fact that the considered perturbations reduce the reactor temperature.

#### 4. Startup Procedure

Simulating the set of equations (2-4) permits to define:

- a procedure for approach to criticality ( $K = 1$ )
- a procedure for bringing the reactor up to power 600 kW.

These procedures are intended as typical insertion rate curves for the uncontrolled reactor (no control, no scram system) and may be considered as the optimum insertion rates meeting the following specifications:

- start from subcritical steady state\*
- approach to criticality as quick as possible
- period  $T_R$  always  $\geq 30$  seconds  $\left( T_R = \frac{\bar{P}}{\frac{d\bar{P}}{dt}} \right)$

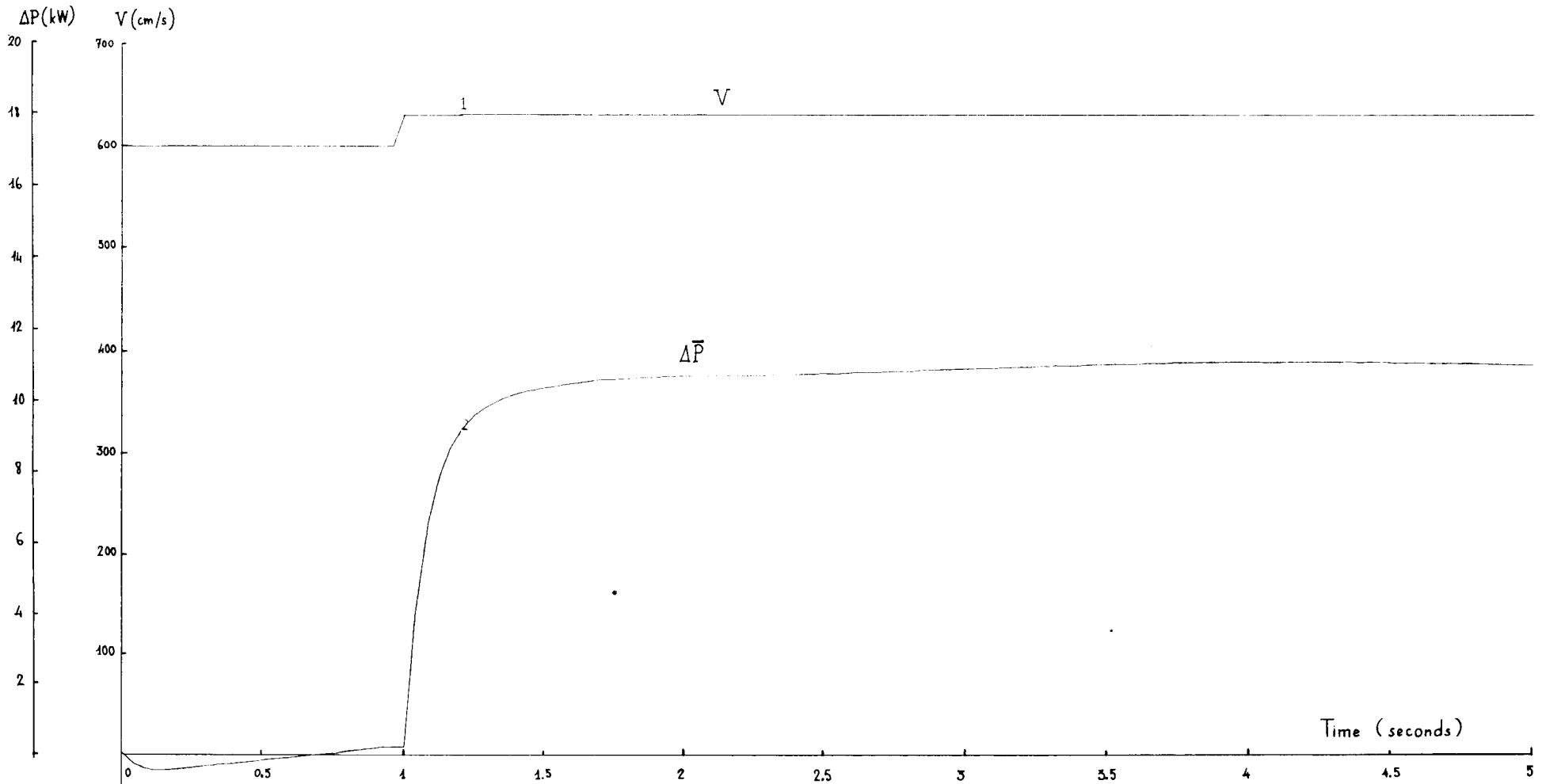
The insertion rates as shown in figure 4 have been found by successively trying numerical values as slopes for  $\epsilon_d$ . Although these results were derived empirically, they give a good first approximation to an optimal startup procedure based on the previous specifications.

Some conclusions coming from this first approach are:

- a) The approach to criticality must be performed very slowly:  
the reactivity insertion must be held in the order of 0,1 pcm/s  
if the period has to be kept  $> 30$  s. With this condition,

---

\* See appendix: Initial Conditions for the Subcritical Steady-State.



RESPONSE TO A CHANGE ON COOLANT VELOCITY  
(UNCONTROLLED REACTOR)

FIG. 3-3

the power level at criticality is reasonably high, that is in the order of 150 mW.

b) The time for bringing the reactor up to power (600 kW) lies in the order of 1000 seconds. This time seems to be the minimum required for starting up to power with the imposed safety condition on the period.

## 5. Linearized Reactor Description

A linearized reactor description is derived in this section which leads to a transfer function for the whole reactor - including kinetics, thermal description and feedback reactivity. In a successive step comparisons are made, on the basis of the reactor response to perturbations, between the set of non-linear equations (2-4) and the derived transfer functions.

### 5-1 Derivation of transfer functions

We start with the set of equations (2-4) and consider small deviations from the pulsed steady state.

#### 5-1-1. Derivation of a transfer function for core-kinetics

Assuming the reactor is at steady state at a certain power level, we will denote by  $\epsilon_{m0}$  the  $\epsilon_m$  value such that  $K(\epsilon_{m0}) = 1$  ( $\epsilon_{m0} = 91,1$  pcm) and consider small reactivity derivations  $\Delta\epsilon_m$  from this value. Then:

$$K(\epsilon_{m0} + \Delta\epsilon_m) - K(\epsilon_{m0}) = \Delta\epsilon_m \cdot \left( \frac{dK}{d\epsilon_m} \right)_{\epsilon_{m0}}$$

which gives the following transfer function:

$$\Delta K(s) = \left( \frac{dK}{d\epsilon_m} \right)_{\epsilon_{m0}} \cdot \Delta\epsilon_m(s)$$

$$\Delta K(s) = 3,1745 \cdot 10^{-2} \cdot \Delta\epsilon_m(s)$$

with  $\Delta\epsilon_m$  expressed in pcm.

In the same manner, considering small deviations from the pulsed steady state, we write the kinetic equations as:

$$\begin{array}{l}
 \text{steady state} \\
 K_0 = 1, \frac{d\bar{C}_{i0}}{dt} = 0
 \end{array}
 \left[ \begin{array}{l}
 \bar{w}_0 = \frac{K_0}{\beta v} \left( \sum_i \lambda_i \bar{C}_i + S_0 \right) \\
 \frac{d\bar{C}_{i0}}{dt} = \beta v \bar{w}_0 - \lambda_i \bar{C}_{i0}
 \end{array} \right]$$
  

$$\begin{array}{l}
 \text{small deviation} \\
 \text{from} \\
 \text{steady state}
 \end{array}
 \left[ \begin{array}{l}
 \bar{w}_0 + \Delta \bar{w} = \frac{K_0 + \Delta K}{\beta v} \left[ \sum_i \lambda_i (\bar{C}_{i0} + \Delta \bar{C}_i) + S_0 \right] \\
 \frac{d}{dt} (\bar{C}_{i0} + \Delta \bar{C}_i) = \beta v (\bar{w}_0 + \Delta \bar{w}) - \lambda_i (\bar{C}_{i0} + \Delta \bar{C}_i).
 \end{array} \right]$$

The second-order term  $\frac{\Delta K}{\beta v} \sum_i \lambda_i \Delta \bar{C}_i$  is neglected. Since at steady state  $K_0 = 1$  and  $\frac{d\bar{C}_{i0}}{dt} = 0$ , one obtains:

$$\Delta \bar{w} = \frac{1}{\beta v} \sum_i \lambda_i \Delta \bar{C}_i + \bar{w}_0 \Delta K$$

$$\frac{d}{dt} (\Delta \bar{C}_i) = \beta v \Delta \bar{w} - \lambda_i \Delta \bar{C}_i$$

This set of equations is Laplace-transformed on both sides; eliminating  $\Delta \bar{C}_i(s)$  the following transfer function is obtained:

$$\frac{\Delta \bar{w}(s)}{\Delta K(s)} = \frac{\bar{w}_0}{1 - \sum_i \frac{\lambda_i}{s + \lambda_i}}$$

In turns, this result is approximated by a one-precursor group model as:

$$\frac{\Delta \bar{w}(s)}{\Delta K(s)} = \bar{w}_0 \frac{s + \lambda}{s} \quad (\text{see Ref. 10})$$

Introducing finally power instead of fission rate, we obtain the following transfer function relating the power variations  $\Delta \bar{P}$  to the reactivity variations  $\Delta \epsilon_m$ :

$$F(s) = \frac{\Delta \bar{P}}{\Delta \epsilon_m} = \bar{P}_0 \left( \frac{dK}{d\epsilon_m} \right)_{\epsilon_{m0}} \cdot \frac{s + \lambda}{s}$$

The numerical value chosen for  $\lambda$  is  $0.08 \text{ sec}^{-1}$ . Then, for the 600 kW power steady state, this gives:

$\frac{\Delta \bar{P}}{\Delta \epsilon_m} = 1,524 \cdot \frac{12,5 \text{ s} + 1}{\text{s}}$
$\Delta \bar{P}$ expressed in kW <span style="float: right;">(5-1-1)</span>
$\Delta \epsilon_m$ expressed in pcm

5-1-2. Derivation of a transfer function for thermal description

Assuming a constant velocity for the coolant, the set of equations (2-2) consists of linear differential equations and may be directly Laplace-transformed. Since the mean fuel temperature and the mean structure temperature are of main interest, we will establish the results for these two temperatures only,

$$\Delta \bar{T}_f = \frac{\left( s C_g + h_{FS} + \frac{h_{sc}}{L h_{sc}} \right) \rho \Delta \bar{P} + \frac{h_{FS} h_{sc}}{1 + \frac{h_{sc}}{2 V C_c}} \Delta T_c, \text{ in}}{s^2 C_f C_g + s \left[ h_{FS} C_g + \left( h_{FS} + \frac{h_{sc}}{1 + \frac{h_{sc}}{2 V C_c}} \right) C_f \right] + \frac{h_{FS} h_{sc}}{1 + \frac{h_{sc}}{2 V C_c}}}$$

$$\Delta \bar{T}_g = \frac{\rho h_{FS} \Delta \bar{P} + \frac{h_{sc}}{1 + \frac{h_{sc}}{2 V C_c}} (s C_f + h_{FS}) \Delta T_c, \text{ in}}{s^2 C_f C_g + s \left[ h_{FS} C_g + \left( h_{FS} + \frac{h_{sc}}{1 + \frac{h_{sc}}{2 V C_c}} \right) C_f \right] + \frac{h_{FS} h_{sc}}{1 + \frac{h_{sc}}{2 V C_c}}}$$

These results may be synthesized as follows:

$$\Delta \bar{T}_f(s) = \frac{A(s)}{B(s)} \cdot \Delta \bar{P}(s) + \frac{C(s)}{B(s)} \cdot \Delta T_{c,in}(s)$$

$$\Delta \bar{T}_g(s) = \frac{D(s)}{B(s)} \cdot \Delta \bar{P}(s) + \frac{E(s)}{B(s)} \cdot \Delta T_{c,in}(s)$$

(5-1-2)

where: (expressing power in kW and temperature in °C)

$$A(s) = (sC_g + h_{Fs} + \frac{h_{sc}}{1 + \frac{Lh_{sc}}{2VC_c}})$$

$$A(s) = 0,22 s + 2,98$$

$$B(s) = s^2 C_f C_g + s \left[ h_{Fs} C_g + \left( h_{Fs} + \frac{h_{sc}}{1 + \frac{Lh_{sc}}{2VC_c}} \right) C_f \right] + \frac{h_{Fs} h_{sc}}{1 + \frac{Lh_{sc}}{2VC_c}}$$

$$B(s) = 3,117 s^2 + 45,176 s + 16,174$$

$$C(s) = \frac{h_{Fs} h_{sc}}{1 + \frac{Lh_{sc}}{2VC_c}}$$

$$C(s) = 16,174$$

$$D(s) = \rho h_{Fs}$$

$$D(s) = 18,535$$

$$E(s) = \frac{h_{sc}}{1 + \frac{Lh_{sc}}{2VC_c}} (sC_f + h_{Fs})$$

$$E(s) = 15,86 s + 16,174.$$

5-1-3. Derivation of a transfer function for feedback reactivity

Since  $\alpha_f$  and  $\alpha_g$  are constant coefficients, we obtain immediately from the set of equations (2-3):

(5-1-3)	$\begin{aligned} \Delta\epsilon_{pf}(s) &= \alpha_f \Delta\bar{T}_f(s) \\ \Delta\epsilon_{pf}(s) &= -0,42 \Delta\bar{T}_f(s) \\ \Delta\epsilon_{pg}(s) &= \alpha_g \Delta\bar{T}_g(s) \\ \Delta\epsilon_{pg}(s) &= -0,80 \Delta\bar{T}_g(s) \\ \Delta\epsilon_p &= \Delta\epsilon_{pf} + \Delta\epsilon_{pg} \end{aligned}$	with $\Delta\epsilon_{pf}$ , $\Delta\epsilon_{pg}$ , $\Delta\epsilon_p$ expressed in pcm $\Delta\bar{T}_f$ and $\Delta\bar{T}_g$ ex- pressed in °C.
---------	---	--

From the previous results, (5-1-1), (5-1-2), (5-1-3) one may build the block-diagram represented in Figure 5-1.

5-2. Comparison between the non-linearized and the linearized reactor description

The block diagram shown in Fig. 5-1 and the relative numerical values may be used to get the reactor response to reactivity or inlet coolant temperature perturbations. However, one must remember that the linearized reactor description holds only for small deviations from a particular steady-state; moreover, all of the numerical values from (5-1-1) to (5-1-3) hold only for the 600 kW steady-state. Therefore, it is of importance to check the validity of this linearization and to know how representative the linearized reactor description is with respect to the set of non-linear equations (2-4).

We considered some increasing steps of reactivity (1,2,3,4,5 pcm) and plotted the obtained power responses:

- a - using the transfer functions.
- b - simulating the complete set of non-linear equations (2-4) by means of the SAHYB programme.

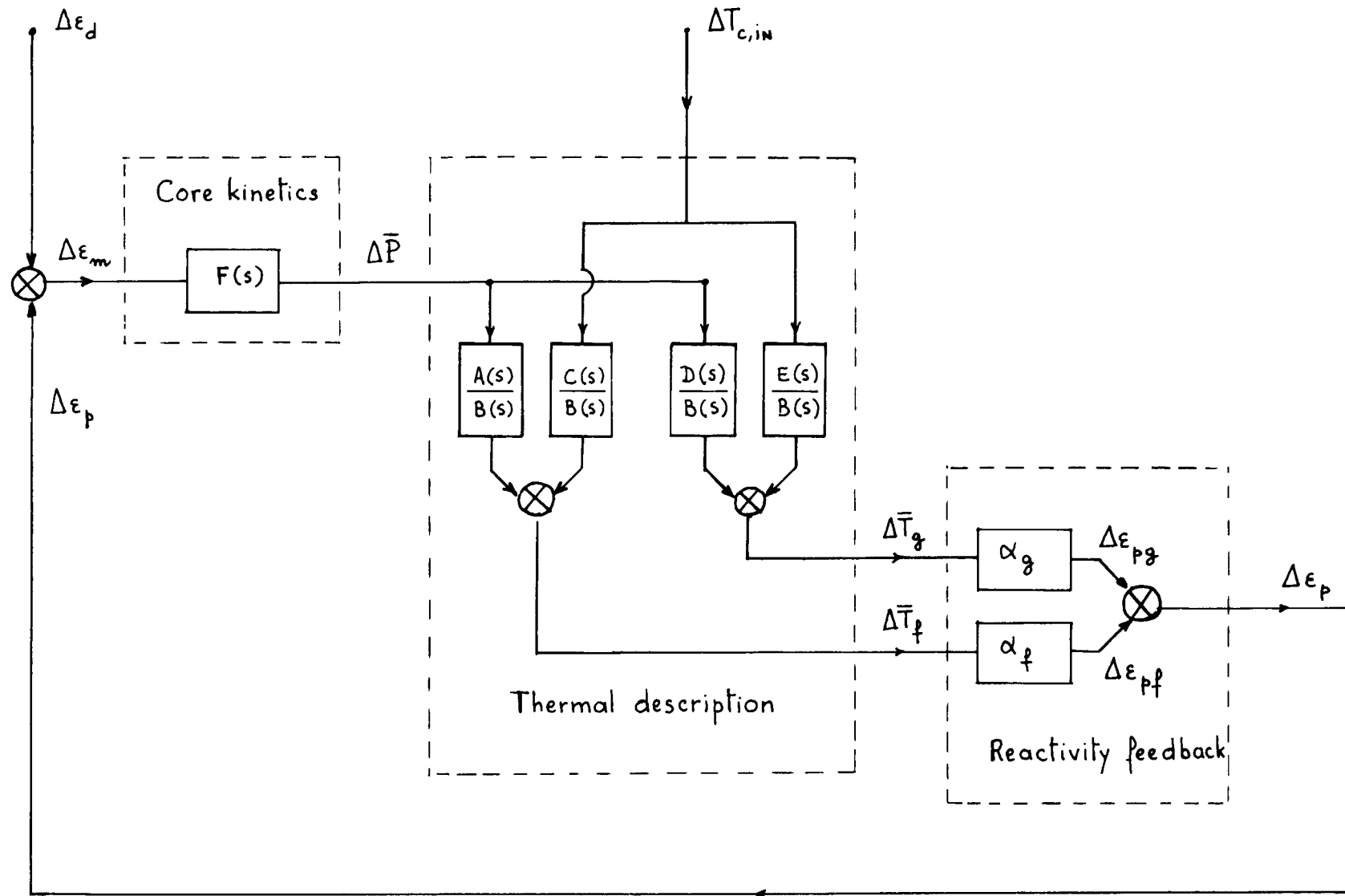


Fig. 5-1.- Linearized reactor description.  
 (holds for small deviations from pulsed steady state)

In the same manner we considered some increasing steps of inlet coolant temperature (1,2,3,4,5 °C) and plotted the power-response for both the two cases.

### 5-2-1. Power response to reactivity perturbations

Assuming  $\Delta T_{c,in} = 0$ , it is found [from the block-diagram represented in figure 5-1, or from the set of results (5-1-1) to (5-1-3)]:

$$\frac{\Delta \bar{P}(s)}{\Delta \epsilon_d(s)} = 19,05 \frac{s^3 + 14,573 s^2 + 0,348 s + 0,415}{s^3 + 15,058 s^2 + 21,946 s + 1,337}$$

The subroutine POLRT (Ref.11) was used to calculate the roots of these polynomial expressions and gave:

$$\frac{\Delta \bar{P}(s)}{\Delta \epsilon_d(s)} = 19,05 \frac{(s+0,08)(s+0,37)(s+14,12)}{(s+0,064)(s+1,56)(s+13,43)}$$

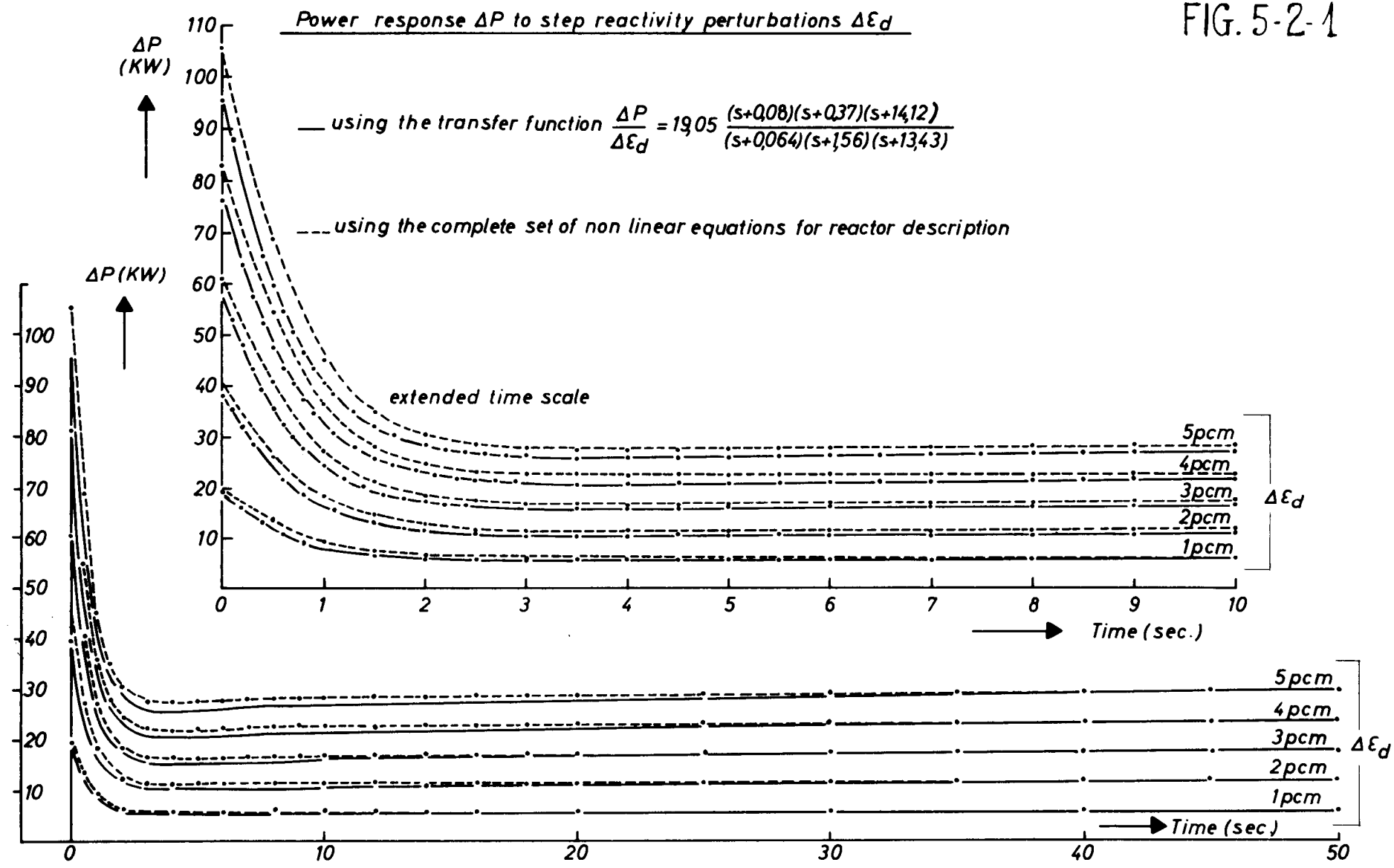
Results are plotted in figure 5-2-1. As is to be expected, the power responses obtained using the transfer function hold good for small perturbations: the more the step height is increased, the less the curves agree. Retaining as good agreement a difference of less than 10 %, it may be seen in figure 5-2-1 that the derived transfer function holds up to about 3 pcm deviation.

It must be pointed out that in these conditions (steps  $\leq 3$ pcm) the transients as well as the final steady states are well contained in the transfer function. If only the final steady states were of interest, the transfer function would hold still higher than 5 pcm - which means that the transfer function might also be used for getting the response to larger slow reactivity deviations.

### 5-2-2. Power response to inlet-coolant temperature perturbations

Assuming now  $\Delta \epsilon_d = 0$ , it is found [from the block-diagram of figure (5-1) or from the set of results (5-1-1) to (5-1-3)]:

FIG. 5-2-1



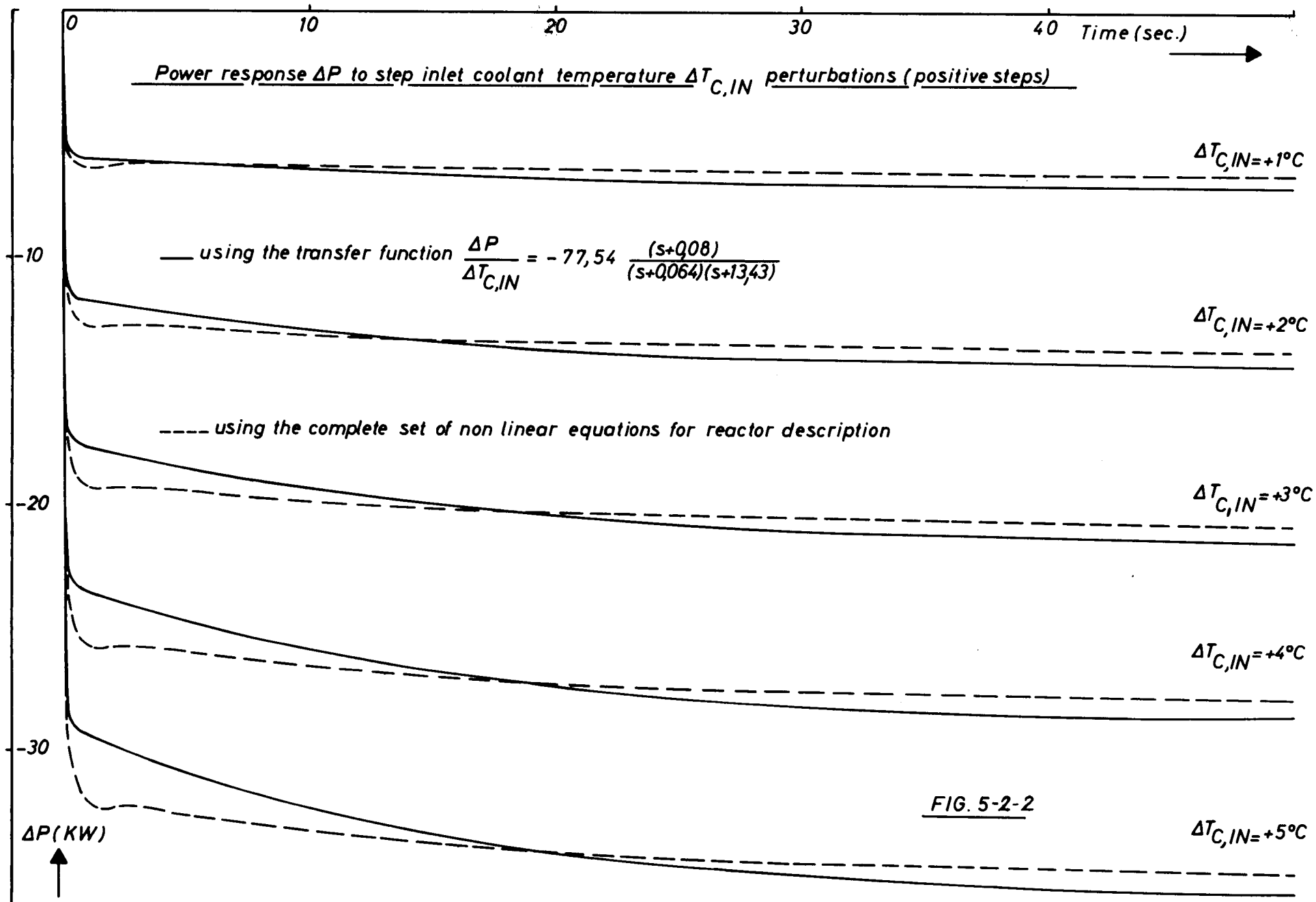


FIG. 5-2-2

$$\frac{\Delta \bar{P}(s)}{\Delta T_{c,in}(s)} = \frac{F(s) (\alpha_f C(s) + \alpha_g E(s))}{B(s) - F(s) (\alpha_f A(s) + \alpha_g D(s))}$$

$$\frac{\Delta \bar{P}(s)}{\Delta T_{c,in}(s)} = - 77,544 \frac{(s+0.08)(s+1.555)}{(s+0.064)(s+1.56)(s+13.43)}$$

which simplifies as indicated in Figure 5-2-2. Results are shown in this figure.

Considering the set of curves of Figure 5-2-2, it may be seen that the transfer function  $\frac{\Delta \bar{P}}{\Delta T_{c,in}}$  is quite a good approximation up to 5 °C (difference between curves less than about 10%).

Remark 1

So far we considered the power response of the reactor against reactivity or inlet coolant temperature perturbations. However, all of the presented results from (5-1-1) to (5-1-3) may be arranged in such a manner that also the fuel temperature or the structure temperature, or any other parameter of interest might be considered as an output of the system. Such a work has been performed and has shown that the transfer functions always constitute a good approximation for the set of non-linear equations (2-4).

Remark 2

For clarity we have considered responses to reactivity and inlet coolant temperature separately. Due to the linearity of results from (5-1-1) to (5-1-3), mixed transfer functions may be derived where reactivity and inlet coolant temperature appear together; consequently, complex perturbations may be considered where reactivity and inlet coolant temperature are varied simultaneously.

## 6. Fast Control System

Clearly it seems unreasonable to define a "fast control system" for the reactor since we deal with mean values for all of the parameters. Such a fast control system should be defined using a discrete-time reactor description (Ref.12) However, it may be thought that the faster is the control system based upon mean values, the easier it will work in the discrete conditions. On the other hand, such a "fast control system" was intended to keep the reactor at the desired power level against small perturbations of reactivity (in the order of some pcm) while a "slow control system" was foreseen against large deviations. In this sense, the set of equations for mean values might be used for a preliminary definition of the control system. We present here (see also Ref. 13 ) a possible way to define a fast control system for such a reactor.

The SORA reactor is equipped with a control rod worth 10 pcm, vertically mounted as described in Ref. 4 and Ref.7 . The so-called fast control rod is a rotating one, directly shafted to a drive motor.

For our purpose it is of primary interest to use a motor meeting the following requirements:

- small time constant to achieve a high rapidity response;
- high rotor inertia with respect to the inertia of the driven mechanism: in this manner the load inertia has a small effect on the motor time constant;
- low nominal speed: in this manner the motor may be shafted directly on the control rod without any gearbox;
- power in the range of 100 W.

In order to meet these general requirements, we chose a torque-motor of the Inland Motor Corporation (Radford, Virginia):

type	T 5135
mechanical time constant	$17 \cdot 10^{-3}$ second
rotor moment of inertia	$3 \cdot 10^{-3}$ lb.ft.sec <sup>2</sup> = $4.05 \cdot 10^{-3}$ kgm <sup>2</sup>
power at peak torque	119 Watt
maximum no-load speed	220 rpm.

As may be seen, when such a motor is linked to the load the overall mechanical time constant changes into:

$$\begin{aligned} & \left( \text{Mechanical time constant} \right)_{\text{of the motor}} \times \frac{(\text{Moment of inertia})_{\text{of the motor}} + (\text{Moment of inertia})_{\text{of the load}}}{(\text{Moment of inertia})_{\text{of the motor}}} \\ & 17 \cdot 10^{-3} \times \frac{4.05 \cdot 10^{-3} + 3.54 \cdot 10^{-4}}{4.05 \cdot 10^{-3}} = 18.5 \cdot 10^{-3} \text{ s.} \end{aligned}$$

Denoting by  $\theta$  the position of the motor shaft (which is also the angular position of the fast control rod) and by  $U$  the voltage applied to the motor, we get as a transfer function between these two parameters (see nomenclature and numerical values):

$$\frac{\theta}{U} = \frac{1}{k} \cdot \frac{1}{s(1 + \tau s + \tau \tau' s^2)}$$

or

$$\frac{\theta}{U} = \frac{1.4652 \cdot 10^4}{s(s+260)(s+73.35)} \quad (6-1)$$

$\theta$  expressed in radians

$U$  expressed in volts.

Now, to synthesize the fast control loop:

a - we will assume the reactor in pulsed steady state condition at 600 kW and use the linearized reactor description holding for small deviations from the previous steady state, i.e.:

$$\frac{\Delta \bar{P}}{\Delta \epsilon_d} = 19.05 \frac{(s+0.08)(s+0.37)(s+14.12)}{(s+0.064)(s+1.56)(s+13.43)} \quad (6-2)$$

- b - we will close the loop and plot a root-locus. (This plot gives direct information about stability and system performances.) From an analysis of this plot the gain will be chosen.
- c - the so-defined fast control system will be added to the set of non-linear equations (2-4) and the obtained overall reactor description will be checked against reactivity perturbations by means of the SAHYB programme.

Steps (a), (b) and (c) will be repeated introducing new elements in the loop to improve the control system performances until satisfactory results are obtained.

#### 6-1. Closing the loop directly

The loop is closed as shown in the block diagram of figure 6-1-1. The fast control system consists of an amplifier of gain  $G$  delivering the voltage  $U$  to the motor described by 6-1; the angular position of the fast control rod is converted into reactivity (10 pcm for  $180^\circ$  angular rotation); this control reactivity is applied to the reactor described by 6-2.

As may be seen, small power demands from the considered state 600 kW are considered and denoted by  $\Delta \bar{P}_0$ ; possible small reactivity perturbations  $\Delta \epsilon_d$  are also considered.

Since we are mainly interested in the whole system response to reactivity perturbations, we will not impose any specification for the response to power demand and assume  $\Delta \bar{P}_0=0$ , which simplifies the system synthesis.

Let us consider now the closed loop transfer function  $\frac{\Delta P}{\Delta \epsilon_d}(s)$ . We obtain directly from the block diagram represented in Figure 6-1-1.

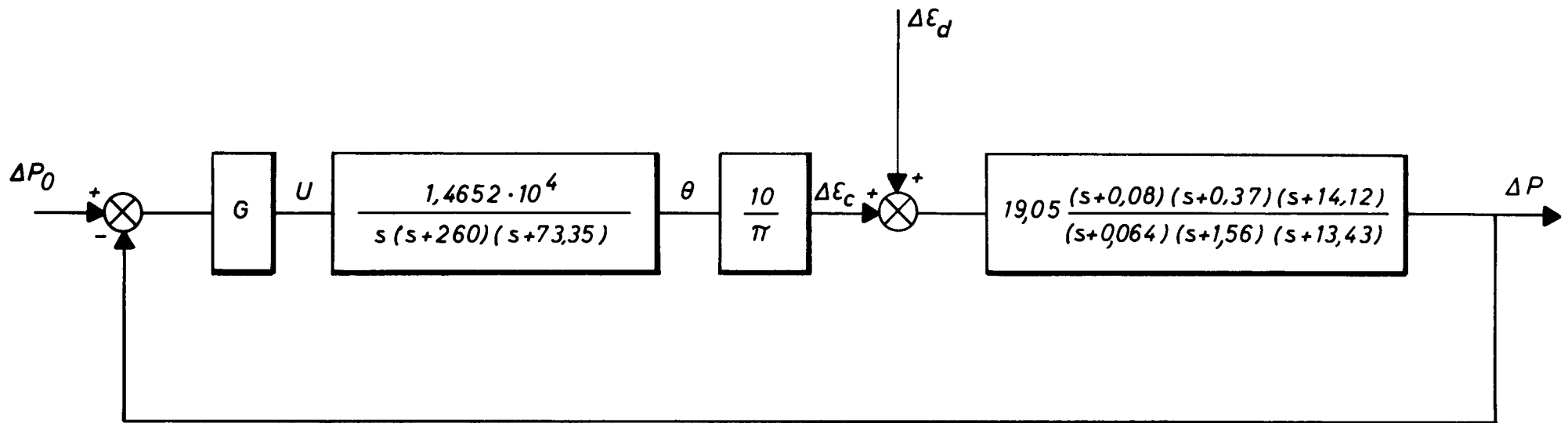
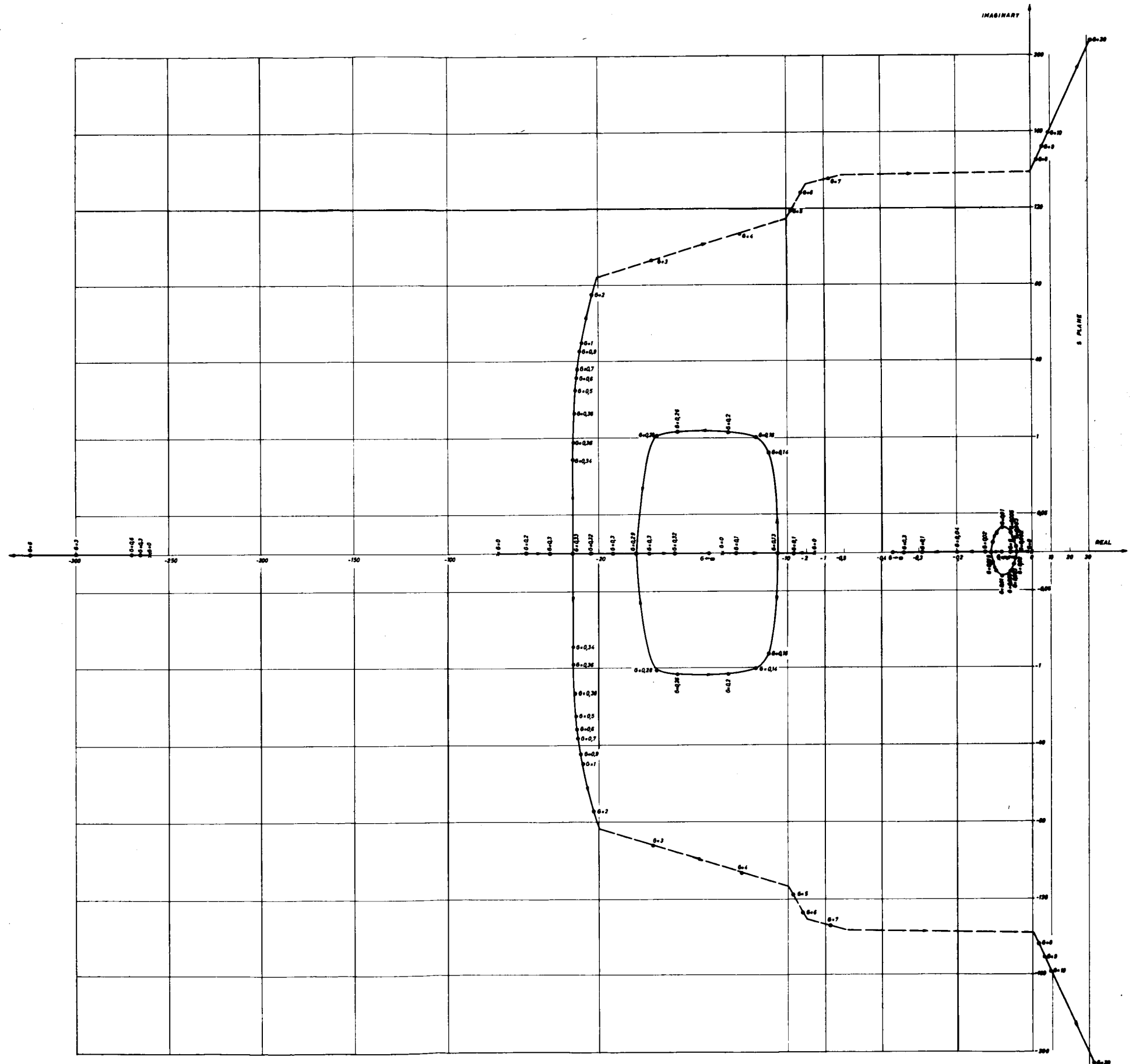


FIG.6-1-1. CLOSING THE LOOP DIRECTLY



ROOT-LOCUS DIAGRAM - STEP 1

FIG. 6.1.2



$$\frac{\Delta \bar{P}}{\Delta \epsilon_d} = \frac{19.05 s(s+0.08)(s+0.37)(s+14.12)(s+73.35)(s+260)}{s(s+260)(s+73.35)(s+0.064)(s+1.56)(s+13.43) + 8.8847 \cdot 10^5 \cdot G(s+0.08)(s+0.37)(s+14.12)}$$

The denominator of this expression contains G as a parameter. Developing and ordering in the successive powers of s we obtain for this denominator a polynomial expression, the roots of which govern the overall stability and the time domain transient response of the system.

A plot of the values of these roots (root-locus) graduated with the corresponding values of G is shown in Fig. 6-1-2. [This root locus was plotted using the subroutine POLRT - Ref.(11).] For G = 0, all of the poles start from the open-loop transfer function poles. As G is increased, they tend to the zeros of the open-loop transfer function or to infinity. So we get three asymptotes: one of them is the real axis, the two others are  $\pm \frac{2\pi}{3}$  from the real axis.

As may be seen, even for small G the poles (crosses) nearer the origin tend quickly to the two nearer zeros (circles). The two further poles meet together, separate, come again to the real axis and separate: one of them tends to the third zero while the other one meets with the fourth pole; these two last separate and become complex. In such a case, choosing a gain G higher than 0.35 results in two control poles - the farthest one starting from - 260 and tending to infinity may be neglected.

We will choose a gain G = 0.6 corresponding to a small overshoot for the step response (for this value of G the system is quite stable and the two control poles are such that imaginary part = real part = 32) and a settling time of about 1/32 second. For such a value of G, the exact roots were calculated always using the subroutine POLRT and led to the following result:

$$\frac{\Delta P}{\Delta \epsilon_d} = \frac{19.05s(s+260)(s+73.35)(s+14.12)(s+0.37)(s+0.08)}{(s+270)(s+14.5)(s+0.354)(s+0.08)(s+31.7+j31.5)(s+31.7-j31.5)}$$

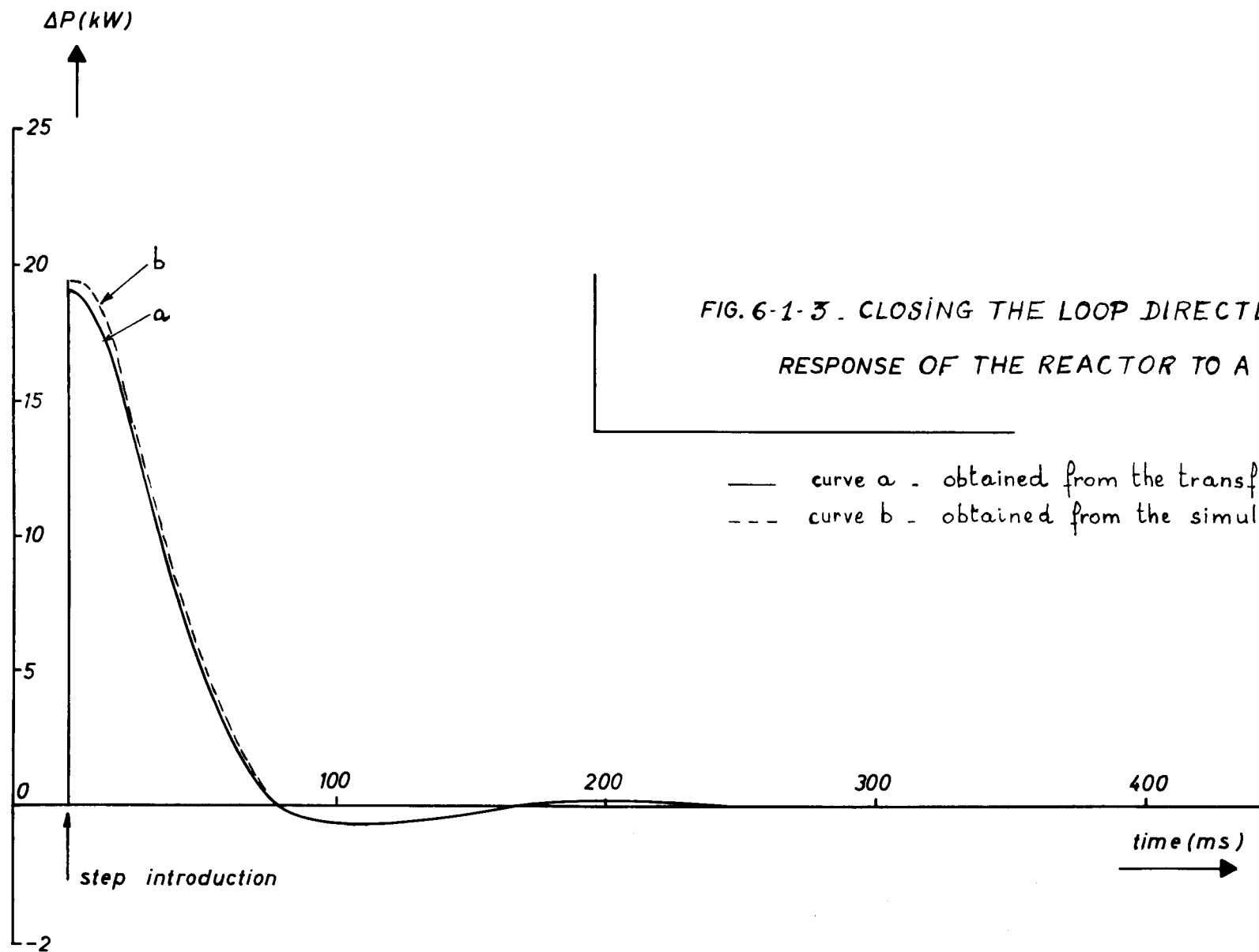


FIG. 6-1-3 . CLOSING THE LOOP DIRECTLY  
 RESPONSE OF THE REACTOR TO A STEP OF 1 pcm

— curve a - obtained from the transfer function  
 --- curve b - obtained from the simulation.

which simplified as:

$$\frac{\Delta P}{\Delta \epsilon_d} = 19.05 \frac{s(s+260)(s+73.35)}{(s+270)(s+31.7+j 31.5)(s+31.7-j 31.5)}$$

This last result, used to plot the power response against a step of reactivity of 1 pcm gave the result shown in Fig. 6-1-3, curve a. From this curve, we see a settling time of about 40 ms and an overshoot less than 5 %, which agrees perfectly with the provisions if one takes into account the simplifications that have been made in obtaining the last transfer function.

At this point we will verify the validity of our treatment by introducing the defined control system into the simulation of the set of non-linear equations (2-4). In other words, we add to the set (2-4) describing the reactor the set of equations describing the control loop, make  $G = 0.6$ , and use the SAHYB program for the simulation. We considered a step of reactivity of 1 pcm and obtained the overall power response shown in Fig. 6-1-3 curve b. A comparison between the two responses (a) and (b) leads to the conclusion that the linearized description used to synthesize the fast control system is more than adequate for our purpose: it may be said that the two responses are coincident.

### 6-2. First improvement of the fast control system performances

A simple means of improving the previous results consists in introducing a tachometer dynamo as a loop around the motor, as shown in the block-diagram of figure 6-2-1. The primary loop is closed exactly as before; a secondary loop is added around the motor. A tachometer dynamo delivering 5 Volt at 100 rpm has been chosen. In terms of transfer function, we introduce the simple block  $0.5 s$  as a feedback around the motor, so that we get now:

$$\frac{\theta}{U} = \frac{1.4652 \cdot 10^4}{s(s+204)(s+130)}$$

With this new (motor and dynamo) description, we will repeat completely the procedure described in § 6-1 and determine the new

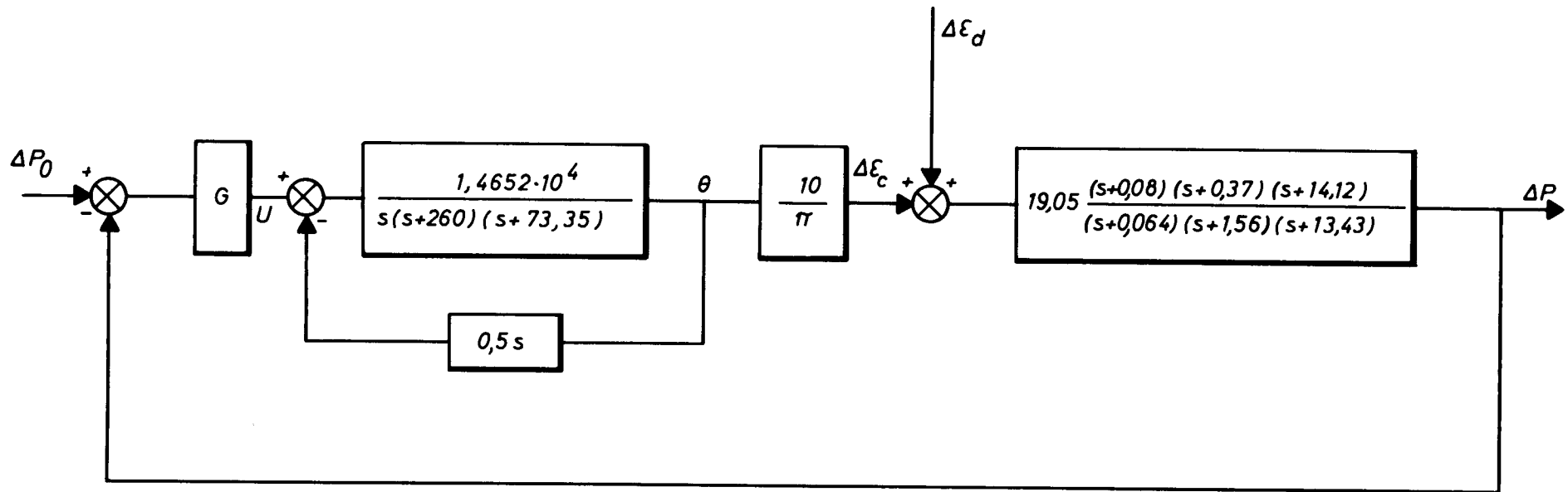


FIG. 6-2-1 . FIRST IMPROVEMENT





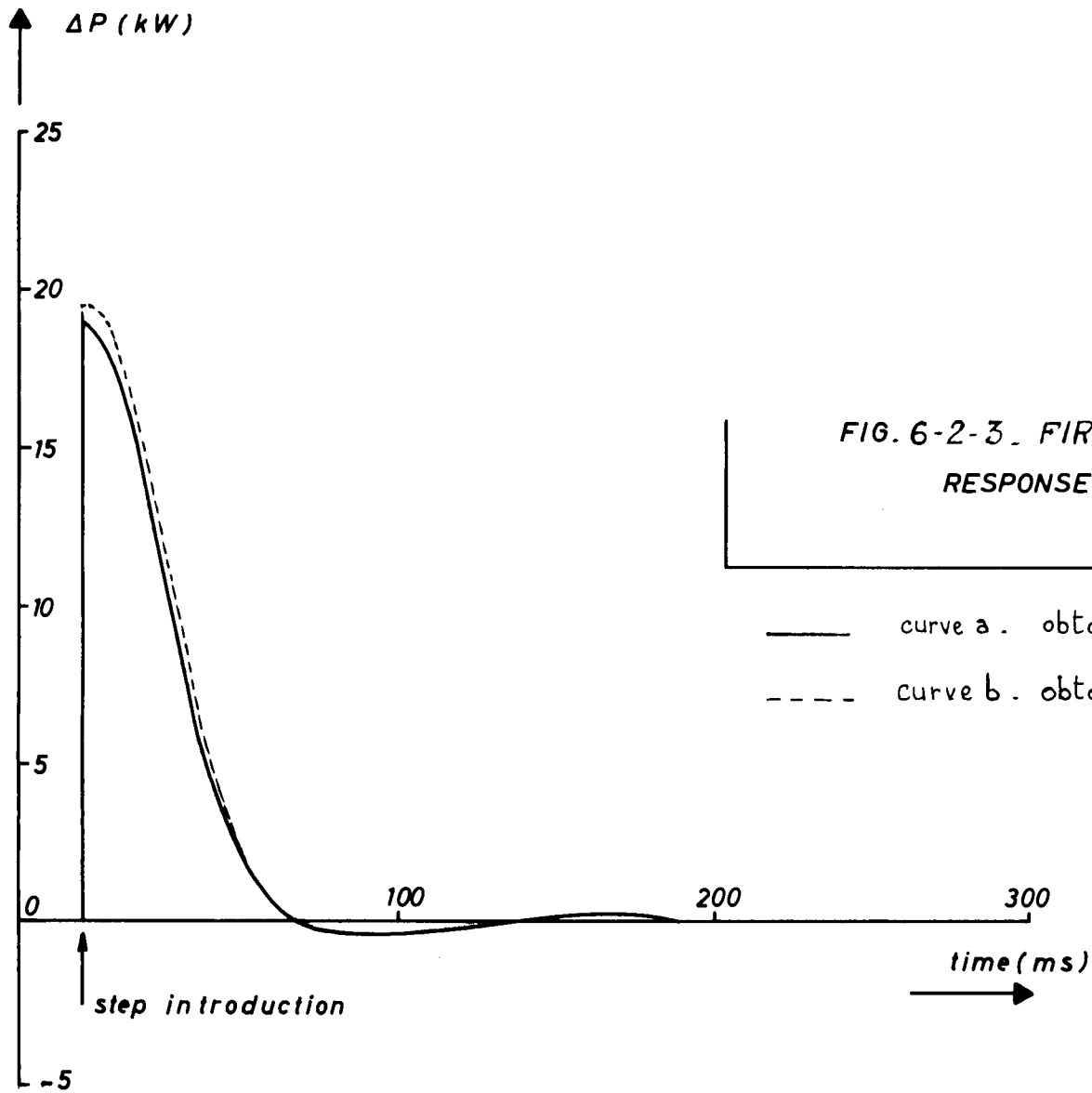


FIG. 6-2-3. FIRST IMPROVEMENT

RESPONSE OF THE REACTOR TO A STEP OF 1 pcm.

— curve a. obtained from the transfer function  
- - - curve b. obtained from the simulation.

value for the gain G.

The overall closed-loop transfer function becomes:

$$\frac{\Delta \bar{P}}{\Delta \epsilon_d} = \frac{19.05 s(s+0.08)(s+0.37)(s+14.12)(s+130)(s+204)}{s(s+204)(s+130)(s+0.064)(s+1.56)(s+13.43) + 8.8847 \cdot 10^5 \cdot G(s+0.08)(s+0.37)(s+14.12)}$$

Developping the denominator, we obtain a polynominal expression which contains G as a parameter. The root-locus for this expression is plotted in Fig. 6-2-2 with the corresponding values of G.

This root-locus is quite similar to the first one: the main difference lies in the fact that the two (symmetric) asymptotic branches start farther from the origin. Choosing as before two complex poles on these branches will result in a quicker transient.

We chose a gain  $G = 1$ , corresponding to a small overshoot in the step-response, a good settling time and a quite safe relative stability.

For  $G = 1$ , the exact roots of the polynomial were calculated and the overall transfer function resulted in:

$$\frac{\Delta P}{\Delta \epsilon_d} = \frac{19.05 s(s+0.08)(s+0.37)(s+14.12)(s+130)(s+204)}{(s+0.0801)(s+0.3572)(s+14.4546)(s+47.8+j38.3) \times (s+47.8-j38.3)(s+238.4)}$$

which simplified as:

$$\frac{\Delta P}{\Delta \epsilon_d} = \frac{19.05 s(s+130)(s+204)}{(s+238.4)(s+47.86+j 38.35)(s+47.86-j 38.35)}$$

This last expression, used to plot the response to a step of reactivity  $\Delta \epsilon_d$  of 1 pcm showed a settling time of about 35 ms and a small overshoot as expected, see fig. 6-2-3, curve a.

Finally, introducing the so defined control system in the simulation and setting the gain at the new value  $G = 1$ , gave the result as shown in fig.6-2-3 curve b. As may be seen from a comparison between figures 6-1-3 and 6-2-3, the performances of the control system are somewhat improved in the second case.

### 6-3. Second improvement of the fast control system performances

The performances obtained as in § 6-2 may still be improved by means of a lead-compensation network. This network would change the arrangement of poles and zeros on the real axis: the operation results in a larger real part of the complex control poles, and thus in a faster response to the perturbations. We will introduce a lead compensation network  $\frac{s+100}{s+500}$  as shown in the block diagram of figure 6-3-1.

We get then for the transfer function of the closed loop:

$$\frac{\Delta P}{\Delta \epsilon_d} = \frac{19.05 s(s+0.08)(s+0.37)(s+14.12)(s+130)(s+204)(s+500)}{\left[ s(s+0.064)(s+1.56)(s+13.43)(s+130)(s+204)(s+500) + 8.8847 \cdot 10^5 \cdot G(s+0.08)(s+0.37)(s+14.12)(s+100) \right]}$$

The root locus for the denominator of this expression is plotted in Fig. 6-3-2, with  $G$  as a parameter. As may be seen this root locus is somewhat different from the previous ones: the two asymptotic branches start much farther from the origin; this time, we have not simply two control poles but another one which tends to  $-100$  as  $G$  is increased.

To get a fast transient response it is of interest to approach this pole  $-100$  with a high gain. On the other hand, a too high gain would bring the complex poles too much on the right and would **slow down** the response. The choice  $G = 10$  is a good compromise for fast response, small undershoot and good stability. It may be seen that for  $G = 10$  we get complex poles with real part = imaginary part.

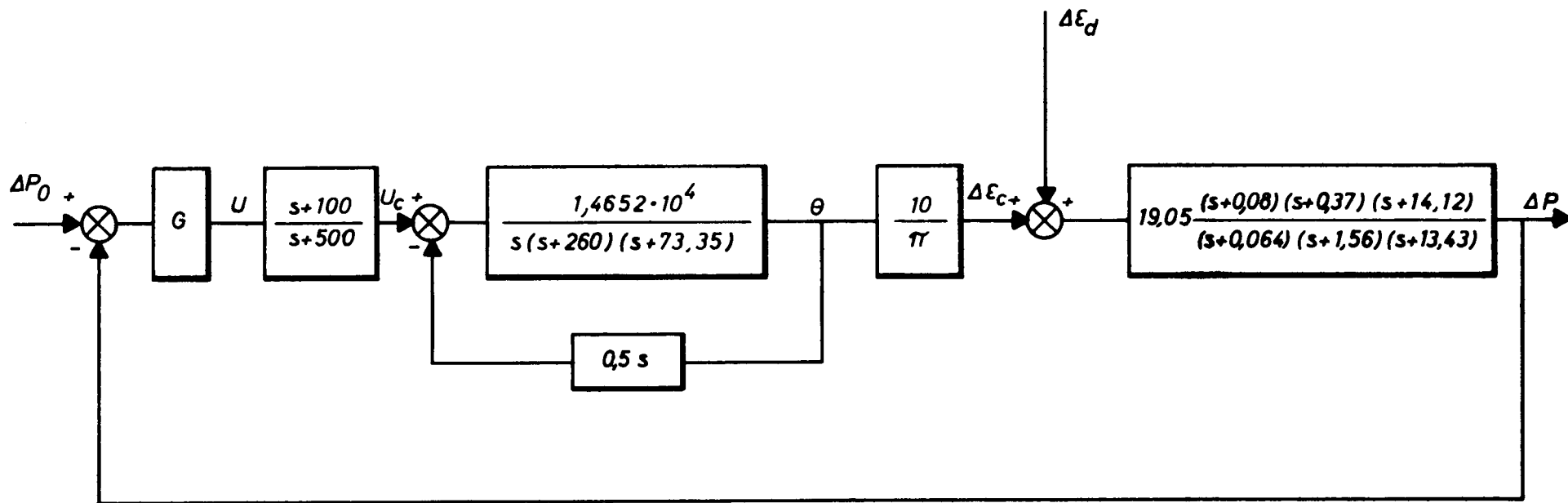
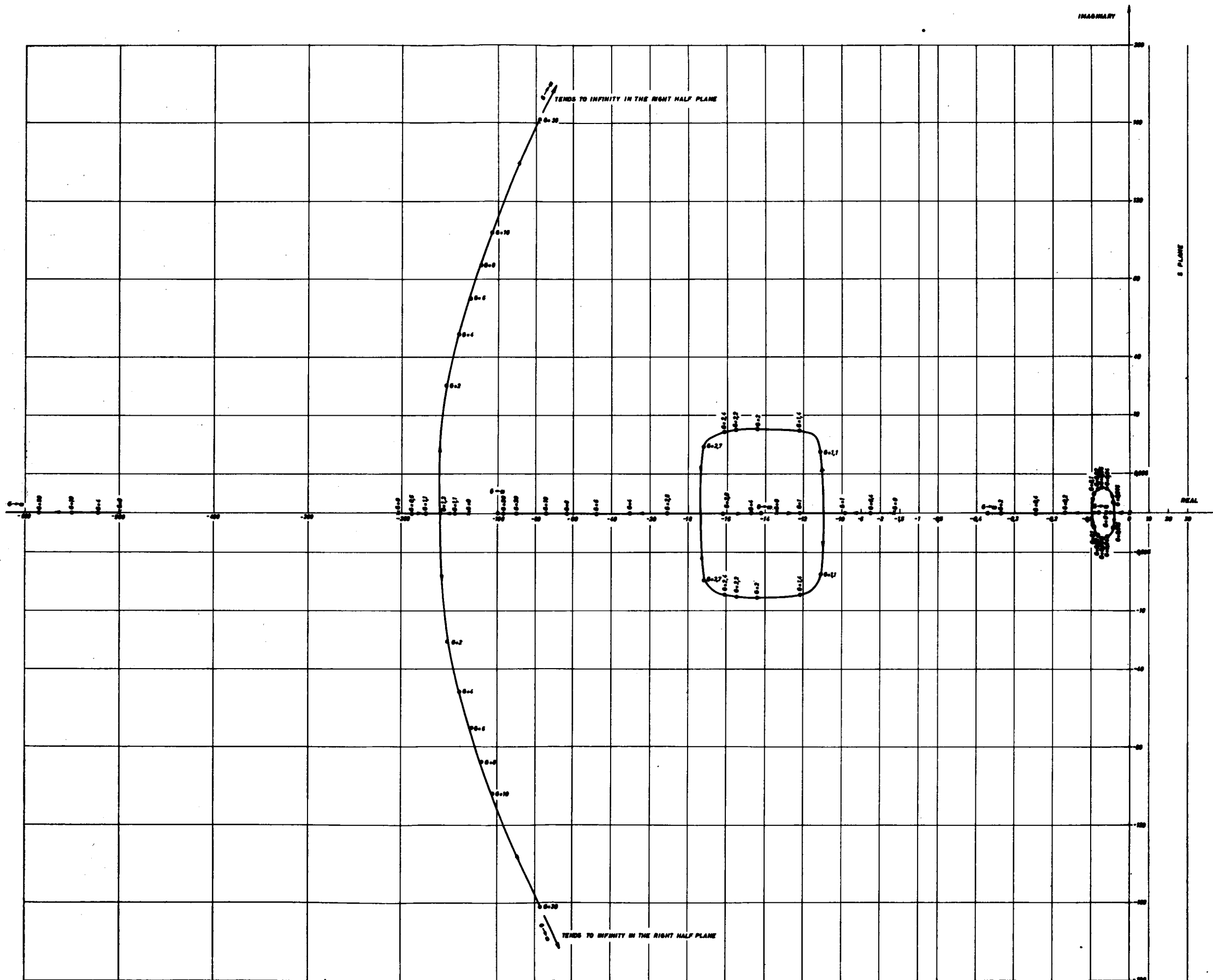


FIG. 6-3-1 . SECOND IMPROVEMENT



ROOT-LOCUS DIAGRAM - STEP 3

FIG. 6.3.2



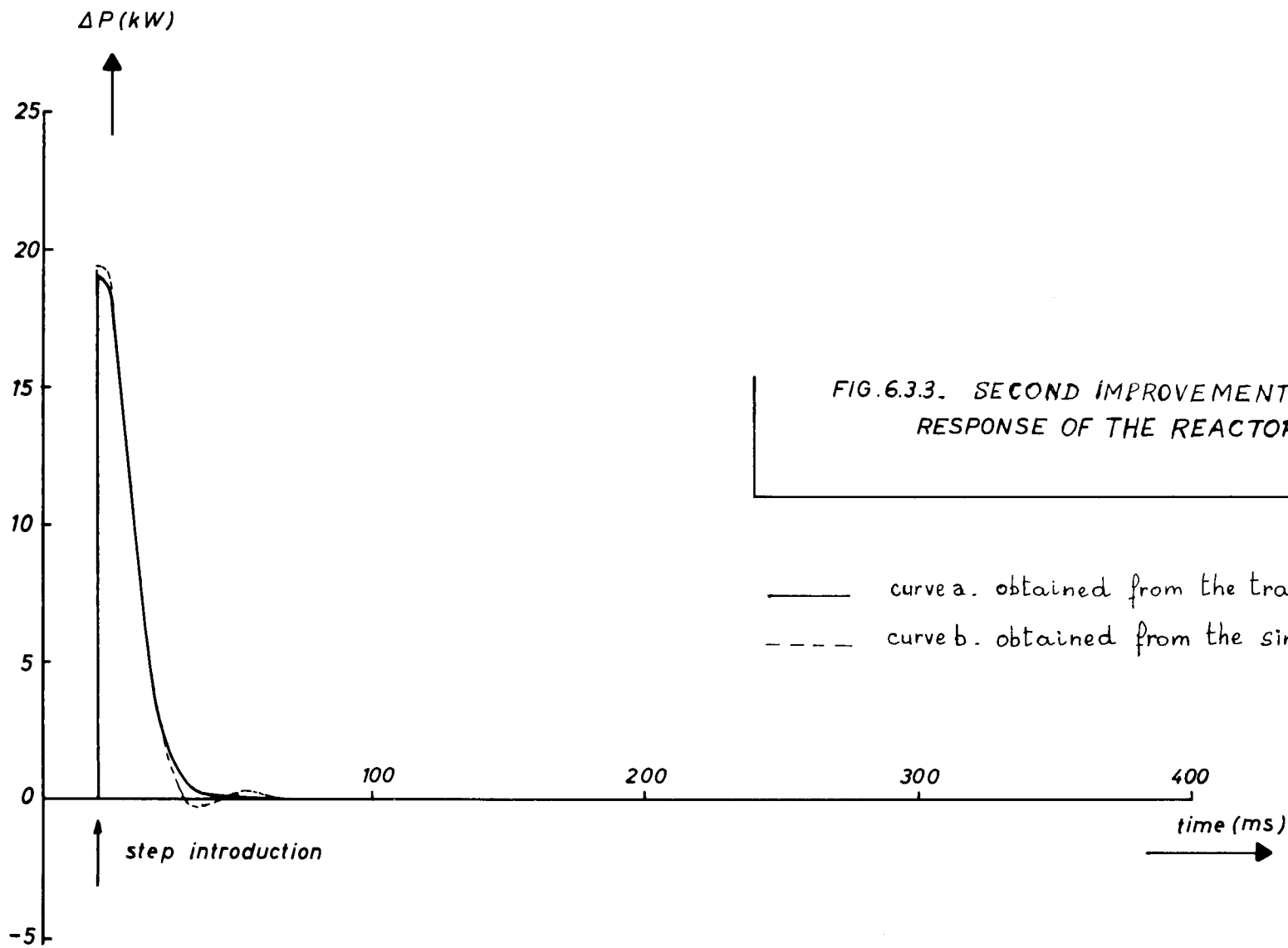


FIG.6.3.3. SECOND IMPROVEMENT  
RESPONSE OF THE REACTOR TO A STEP OF 1 pcm

— curve a. obtained from the transfer function  
 - - - curve b. obtained from the simulation.

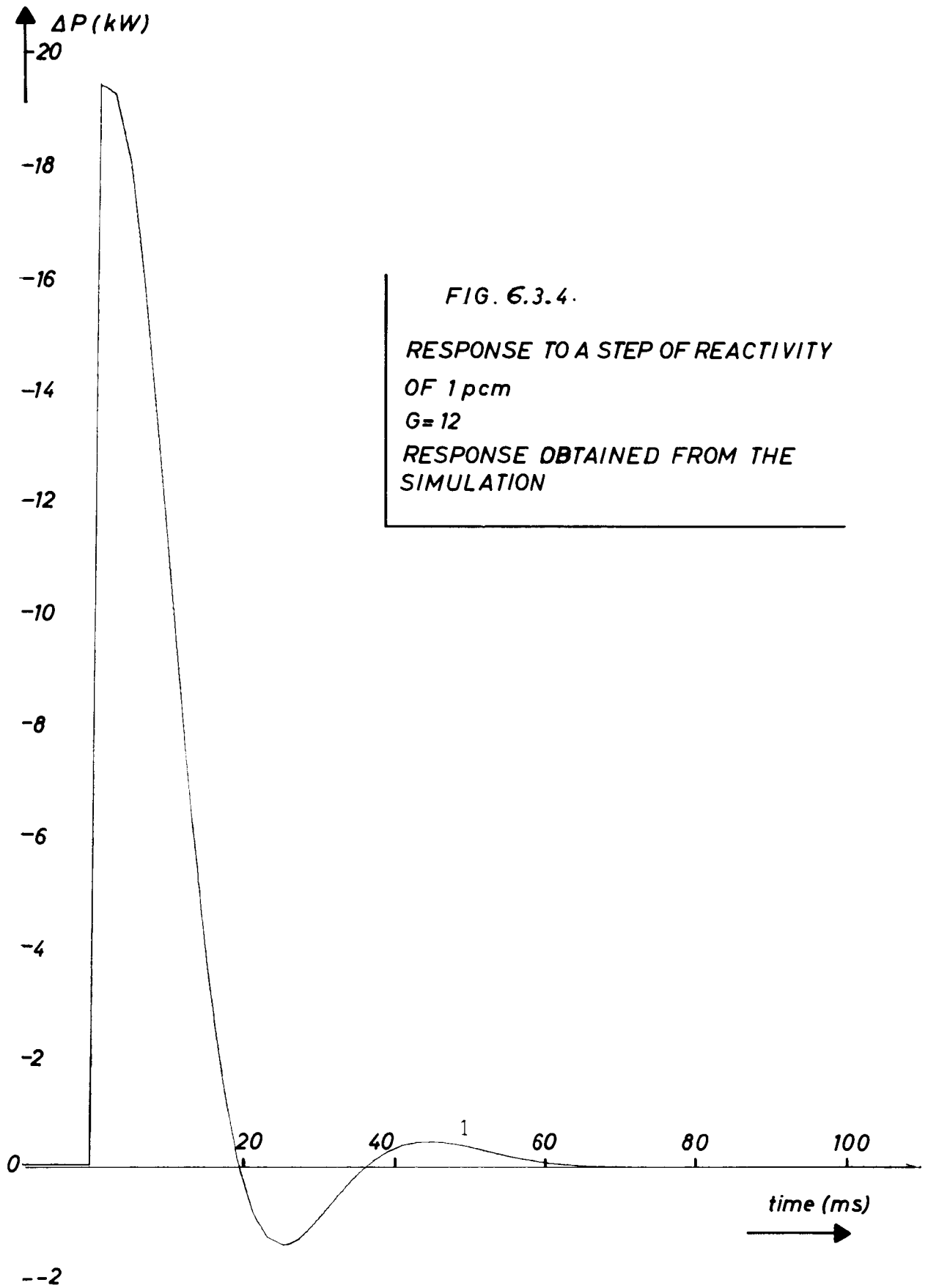


FIG. 6.3.4.  
RESPONSE TO A STEP OF REACTIVITY  
OF 1 pcm  
G = 12  
RESPONSE OBTAINED FROM THE  
SIMULATION

The settling time results from the combination of these two poles and of the third one which tends to -100. For the chosen gain  $G = 10$ , the exact roots of the denominator were found and gave for the transfer function the already simplified expression:

$$\frac{\Delta \bar{P}}{\Delta \epsilon_d} = 19.05 \frac{s(s+130)(s+204)(s+500)}{(s+74.46)(s+550)(s^2+210s + 21816)}$$

Let us now see how this final control system works when added to the set of equations (2-4). Once again the SAHYB program was used for the simulation; a step of reactivity of 1 pcm was introduced as a perturbation. The response of the overall system (reactor + fast control system such as synthesized in this paragraph) is shown in figure 6-3-3. As it may be seen, the fast control system performances are considerably improved with respect to the two first results 6-1-3 and 6-2-3.

One might think that increasing still the gain would lead to a better response. However, the response presents some oscillations as shown in Fig. 6-3-4 which was plotted with  $G = 12$ .

#### 6-4. Basic set of equations for the controlled reactor -

##### Conclusion

As a first conclusion, an important one, all of the results show that the SORA reactor is controllable, although the fast control system synthesis was based upon a set of equations for "mean values"; only the performances of the control system will change a little bit with respect to the real case, due to the sampling effect on the power - in terms of automatic control, the power will be "sampled and hold" at the frequency of the pulsation device.

Major improvements were not investigated, since the obtained settling time lies in the order of 20 ms, which is the smallest time interval that one might take under consideration, always due to the validity of the set of equations (2-4).

As concerns the feasibility of such a control system, some difficulties arise if perturbations really occur under the form of step-functions as we assumed until now, since saturation phenomena (on the amplifier, on the motor) would occur reducing the indicated performances. However, it seems more reasonable from a practical point of view to expect perturbations in the form of "ramp-functions". The situation is then quite sure; the simulation showed that the so-defined control system worked well with ramp-functions until about 50 pcm/second, which is far above expected ramp rates [a response to this type of perturbation is shown in Fig. 6-4-1].

Basic set of equations for the controlled reactor.

- $\epsilon_c$  = control reactivity
- $\epsilon_d$  = input reactivity signal
- $\epsilon_p$  = feedback reactivity
- $\epsilon_m$  = total reactivity

core kinetics	$K = 0.229 + 8.80 \epsilon_m + 0.0176 e^{4140 \epsilon_m}$ $\bar{w} = \frac{K}{\beta v} \left( \sum_i \lambda_i \bar{C}_i + S_0 \right)$ $\frac{d\bar{C}_i}{dt} = \beta_i v \bar{w} - \lambda_i \bar{C}_i$ $\bar{P} = \frac{\bar{w}}{C_f}$
Thermal description	$C_f \frac{d\bar{T}_f}{dt} = \rho \bar{P} - h_{FS} (\bar{T}_f - \bar{T}_g)$ $C_g \frac{d\bar{T}_g}{dt} = h_{FS} (\bar{T}_f - \bar{T}_g) - \frac{h_{sc}}{1 + \frac{h_{sc}}{2VC_c}} (\bar{T}_g - T_{C,IN})$

$$\begin{array}{l}
 \left[ \begin{array}{l}
 T_{c,out} = T_{c,in} + \frac{2}{2VC_c} \frac{1}{1+Ih_{sc}} (\bar{T}_g - T_{c,in}) \\
 T_c = \frac{1}{2} (T_{c,in} + T_{c,out})
 \end{array} \right. \\
 \\
 \left[ \begin{array}{l}
 \epsilon_{pf} = \alpha_f (\bar{T}_f - T_{REF}^*) \\
 \epsilon_{pg} = \alpha_g (\bar{T}_g - T_{REF}^*) \\
 \epsilon_p = \epsilon_{pf} + \epsilon_{pg}
 \end{array} \right. \\
 \\
 \left[ \begin{array}{l}
 U = G(\bar{P}_o - \bar{P}) \\
 \\
 \frac{dU_c}{dt} = \frac{dU}{dt} + \omega_1 U - \omega_2 U_c \\
 U_c - \eta \frac{d\theta}{dt} = k \frac{d\theta}{dt} + \frac{RJ}{k} \frac{d^2\theta}{dt^2} + \frac{J}{k} \frac{d^3\theta}{dt^3} \\
 \\
 \epsilon_c = r\theta
 \end{array} \right.
 \end{array}
 \tag{6-4}$$

Typical responses of the controlled reactor to perturbations are shown in figures 6-4-1, 6-4-2, 6-4-3, 6-4-4.

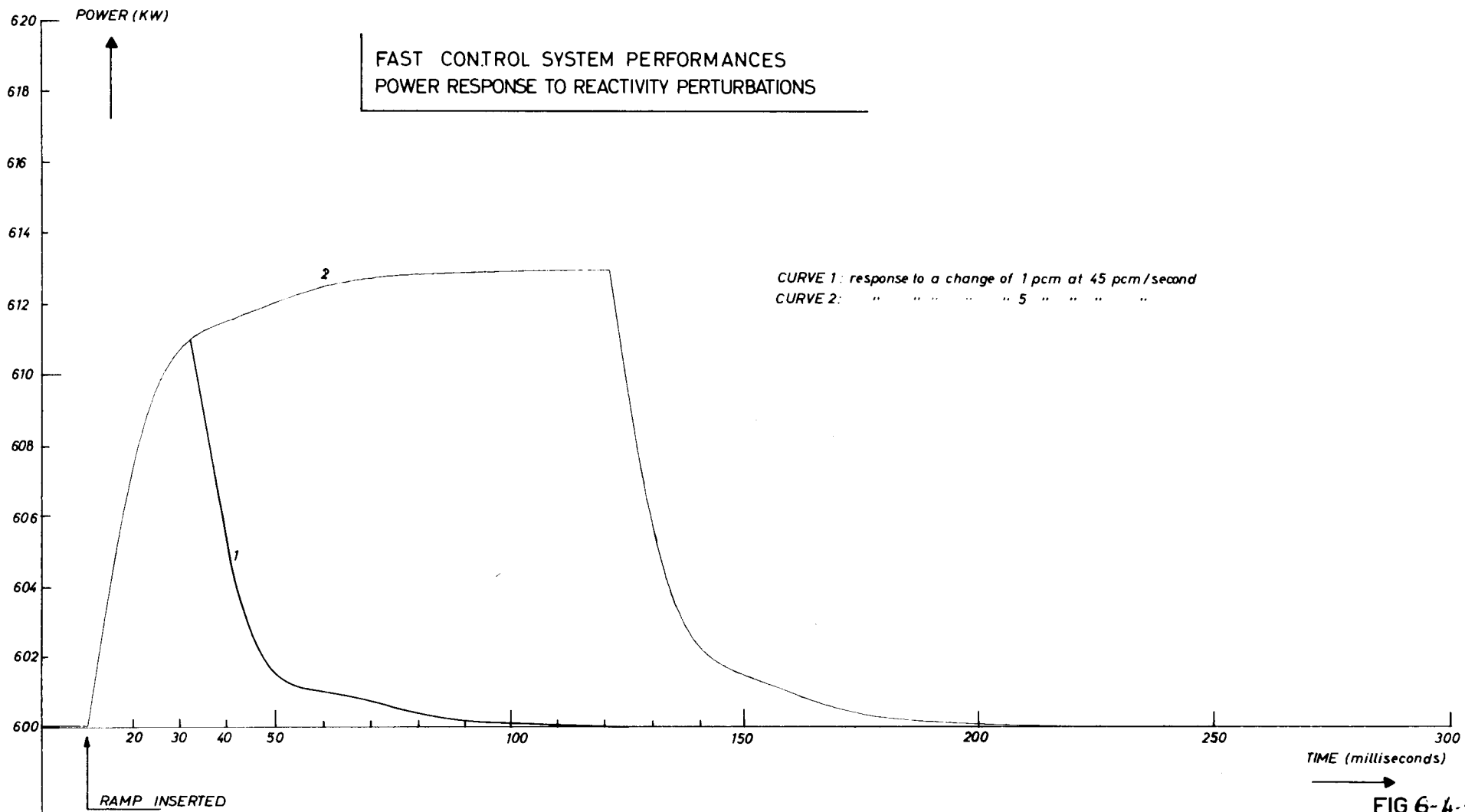


FIG. 6-4-1

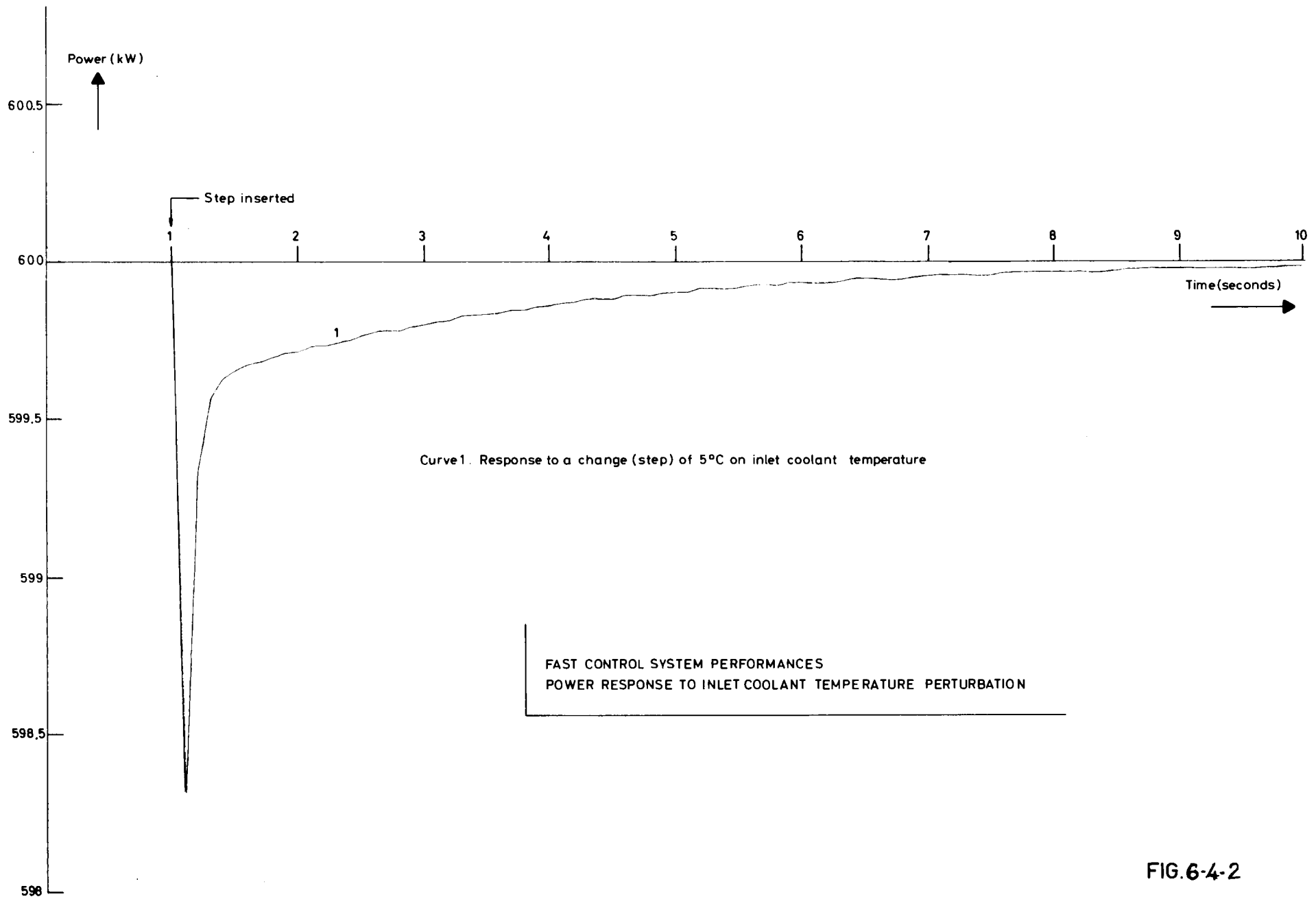


FIG.6-4-2

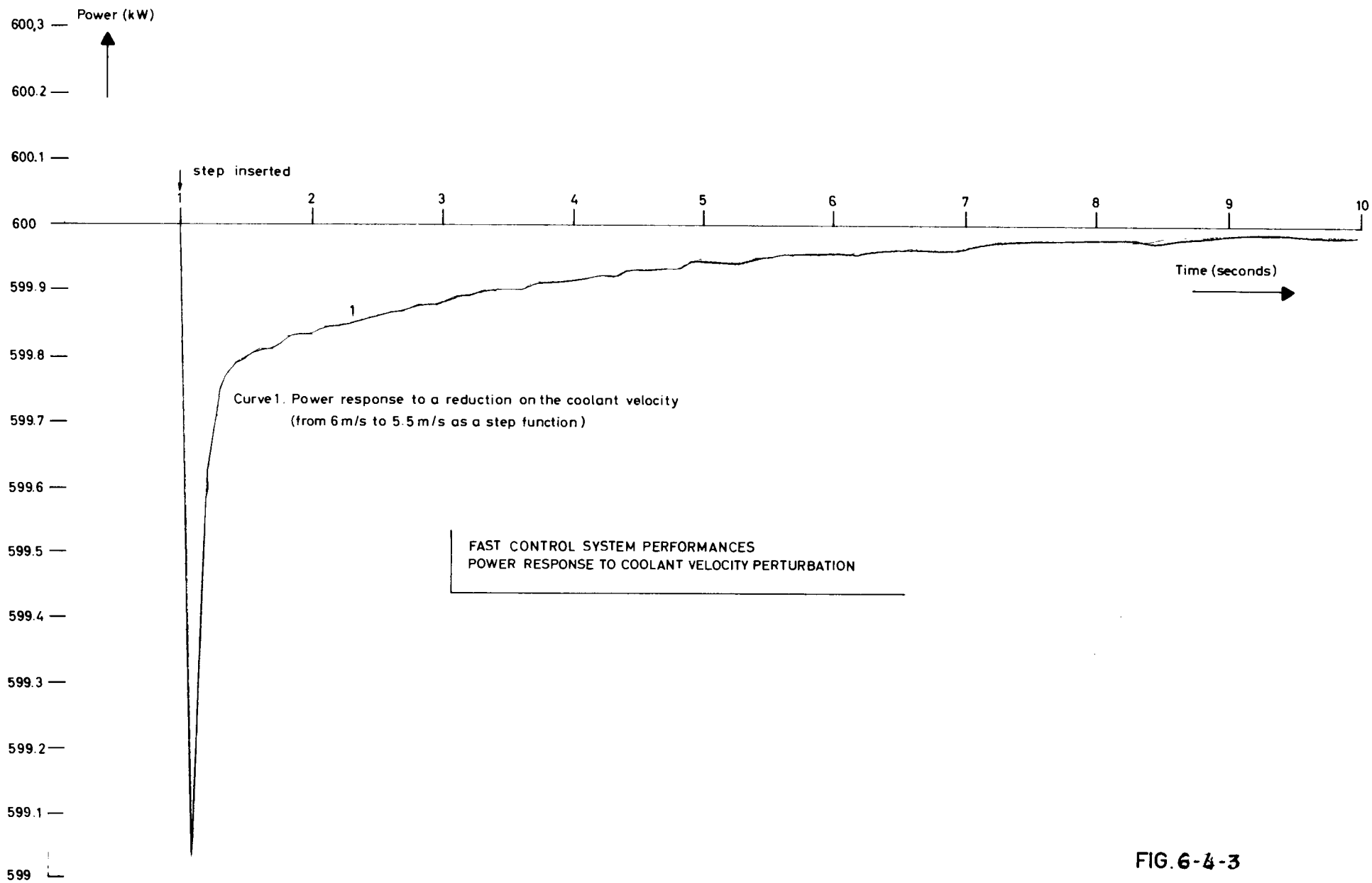
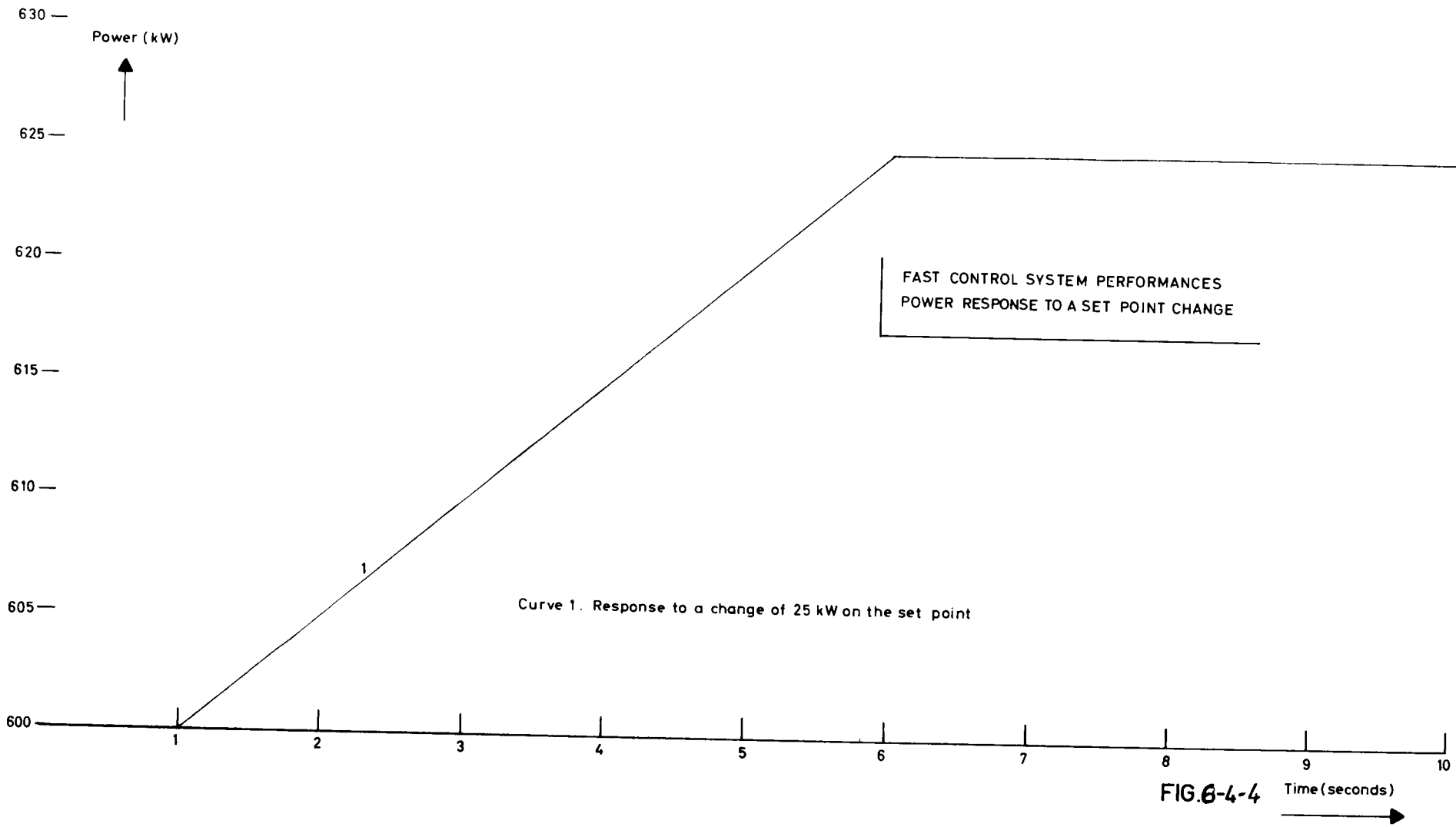


FIG. 6-4-3



7. Malfunctions

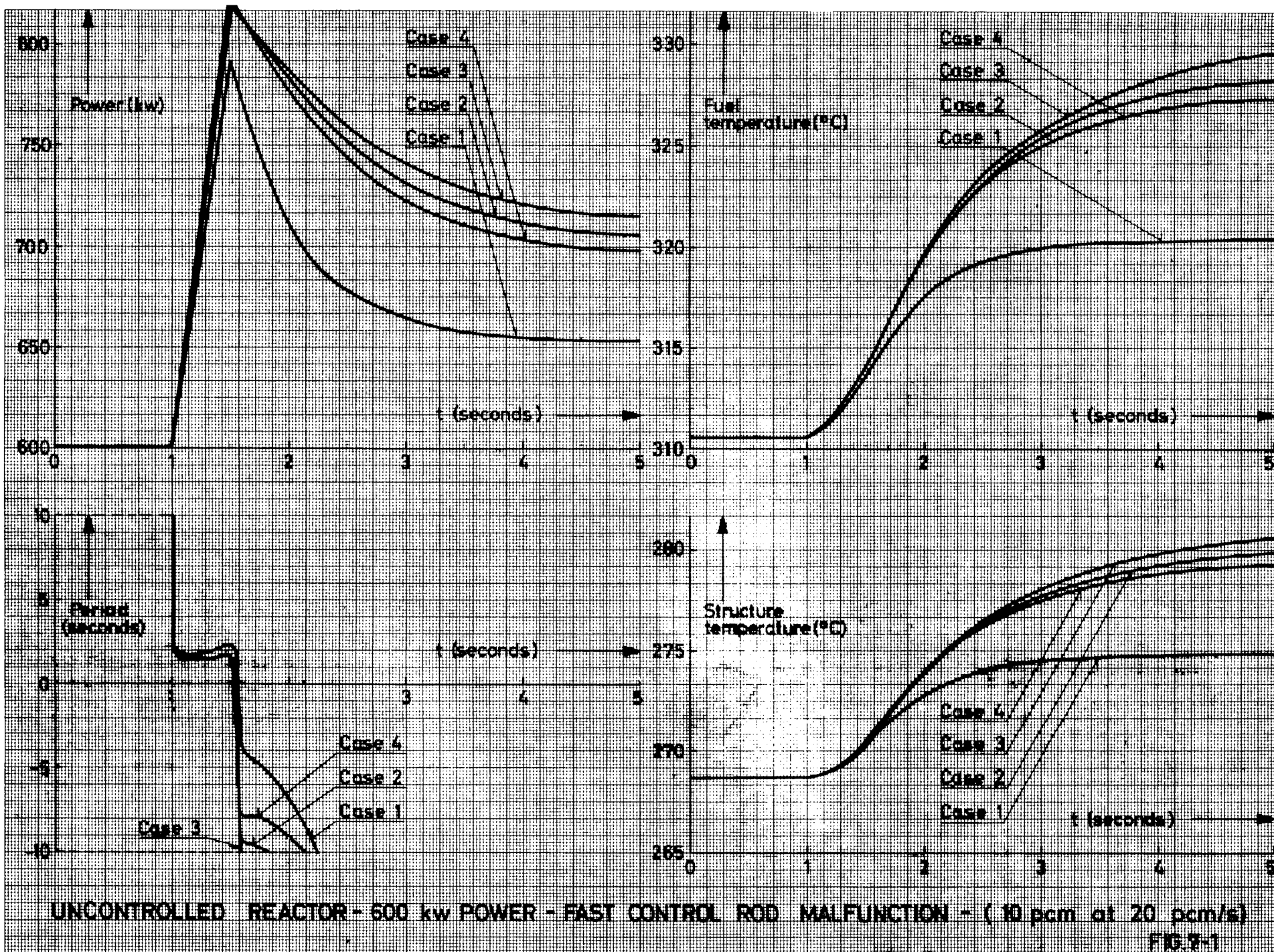
Control rod malfunctions occurring in the uncontrolled reactor have been simulated as a part of reactor safety studies. The set of equations (2-4) was used for this purpose. We investigated the malfunctions of:

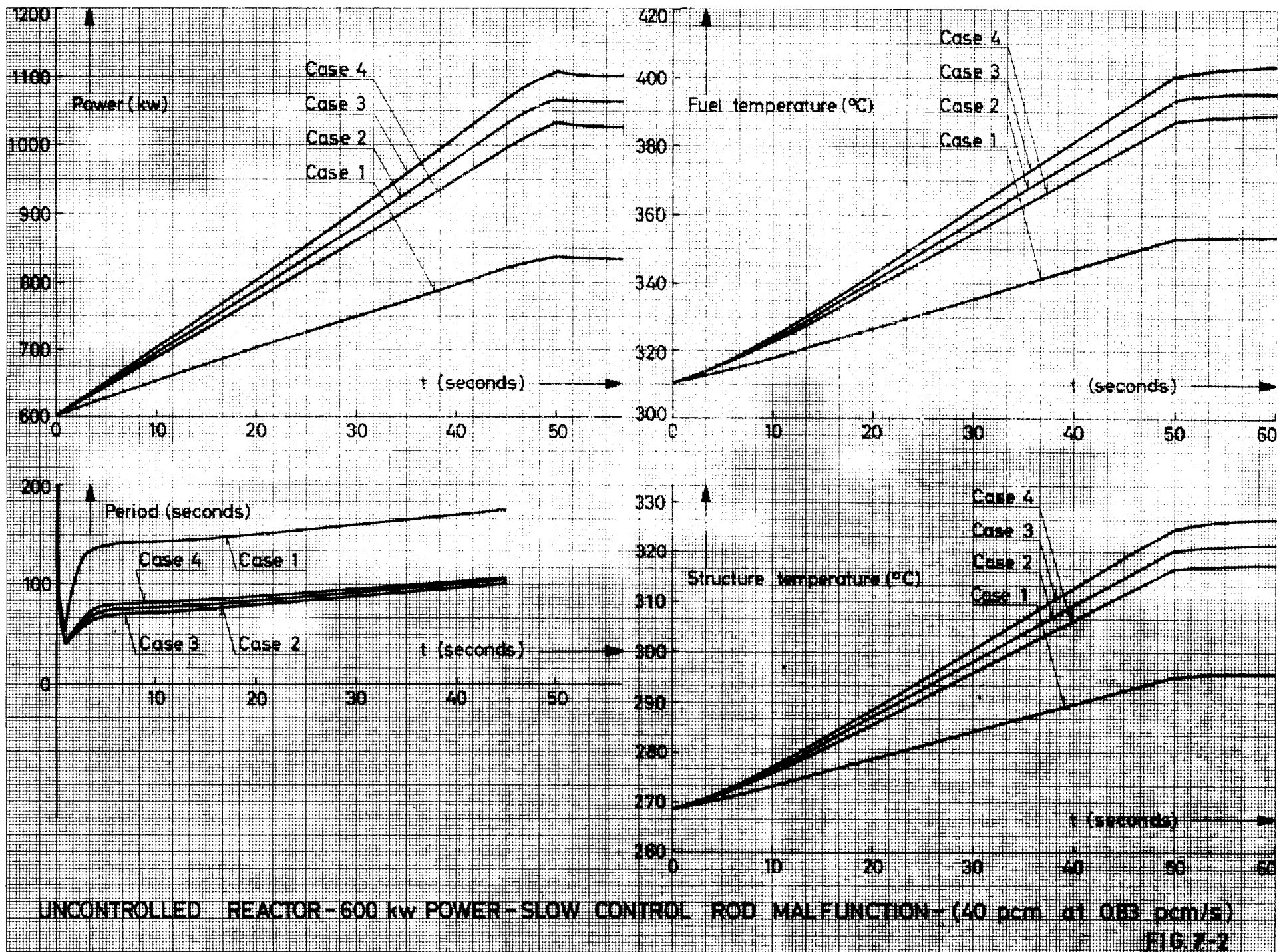
- the fast control rod (by inserting 10 pcm at 20 pcm/s)
- the slow control rod (by inserting 40 pcm at 0.83 pcm/s)
- the regulation rod (by inserting 300 pcm at 3 pcm/s).

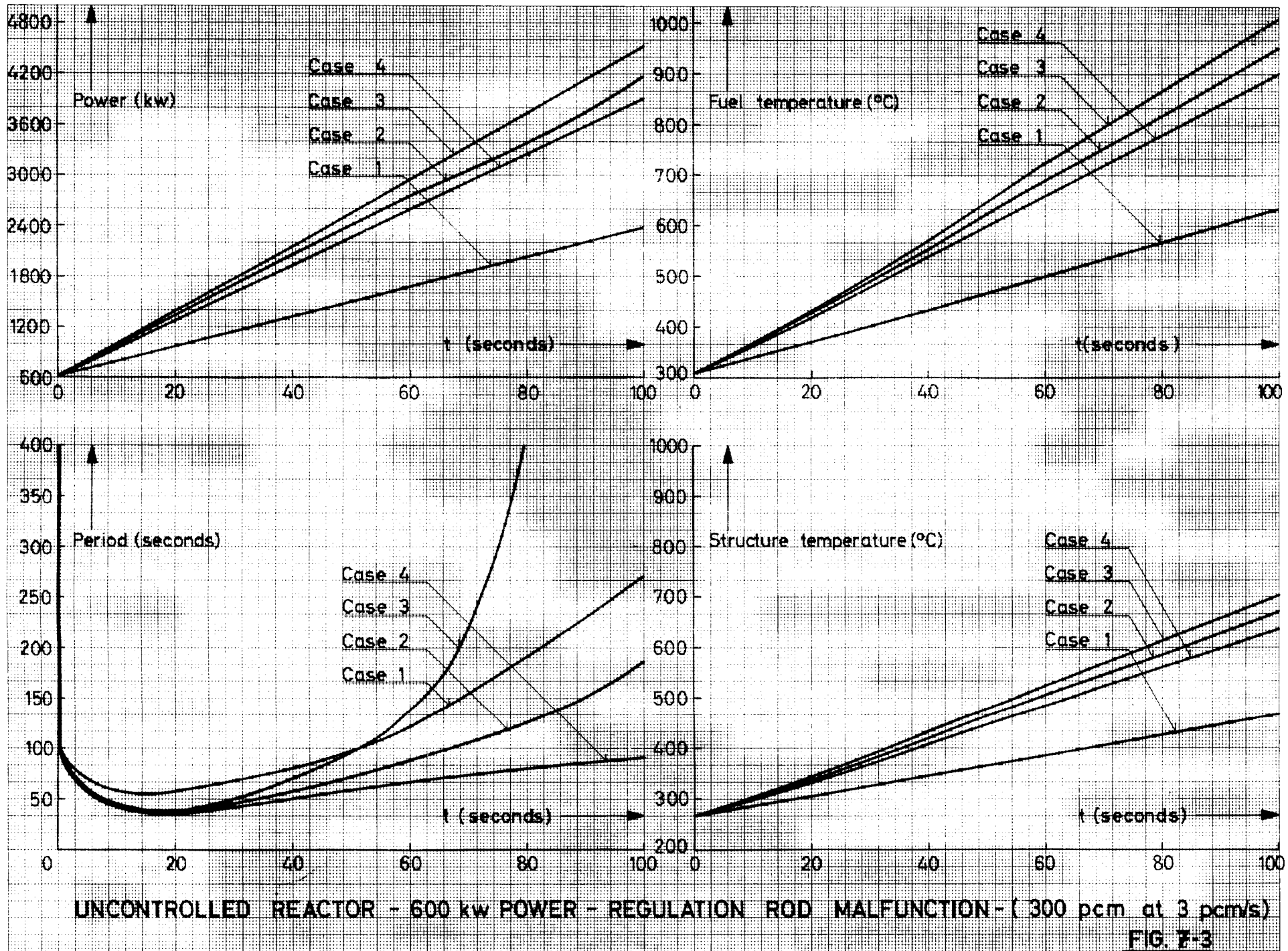
Now, in order to have a first assessment of the importance of a reduction in the values of the reactivity feedback coefficients, each malfunction was repeated changing these coefficients. Four cases were considered:

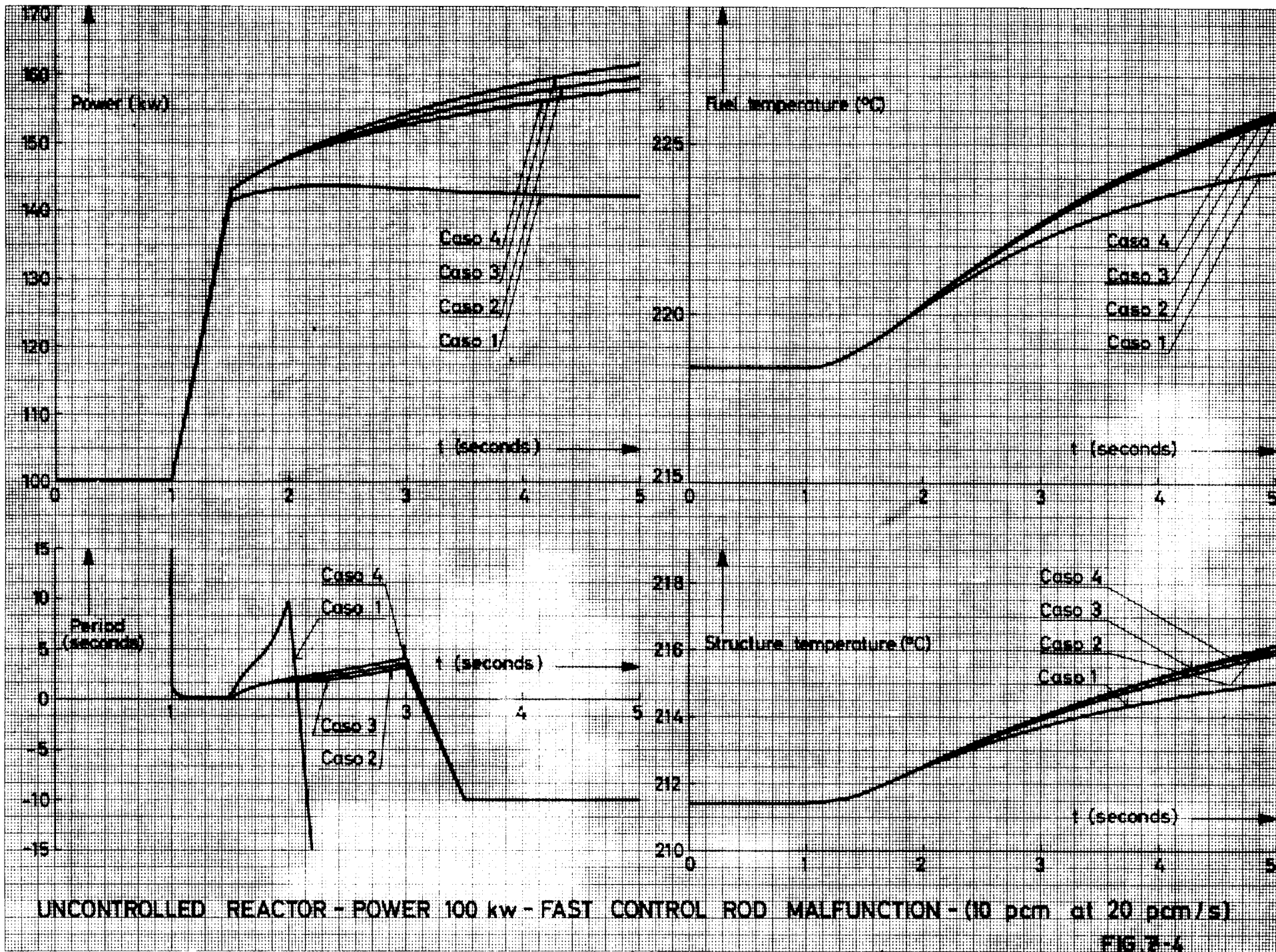
	$\alpha_f$	$\alpha_g$
Case 1	Reference value (-0.42pcm/°C)	Reference value (-0.80pcm/°C)
Case 2	Half reference value (-0.21pcm/°C)	Half reference value (0.40pcm/°C)
Case 3	Reference value (-0.42pcm/°C)	0
Case 4	0	Reference value (-0.80pcm/°C)

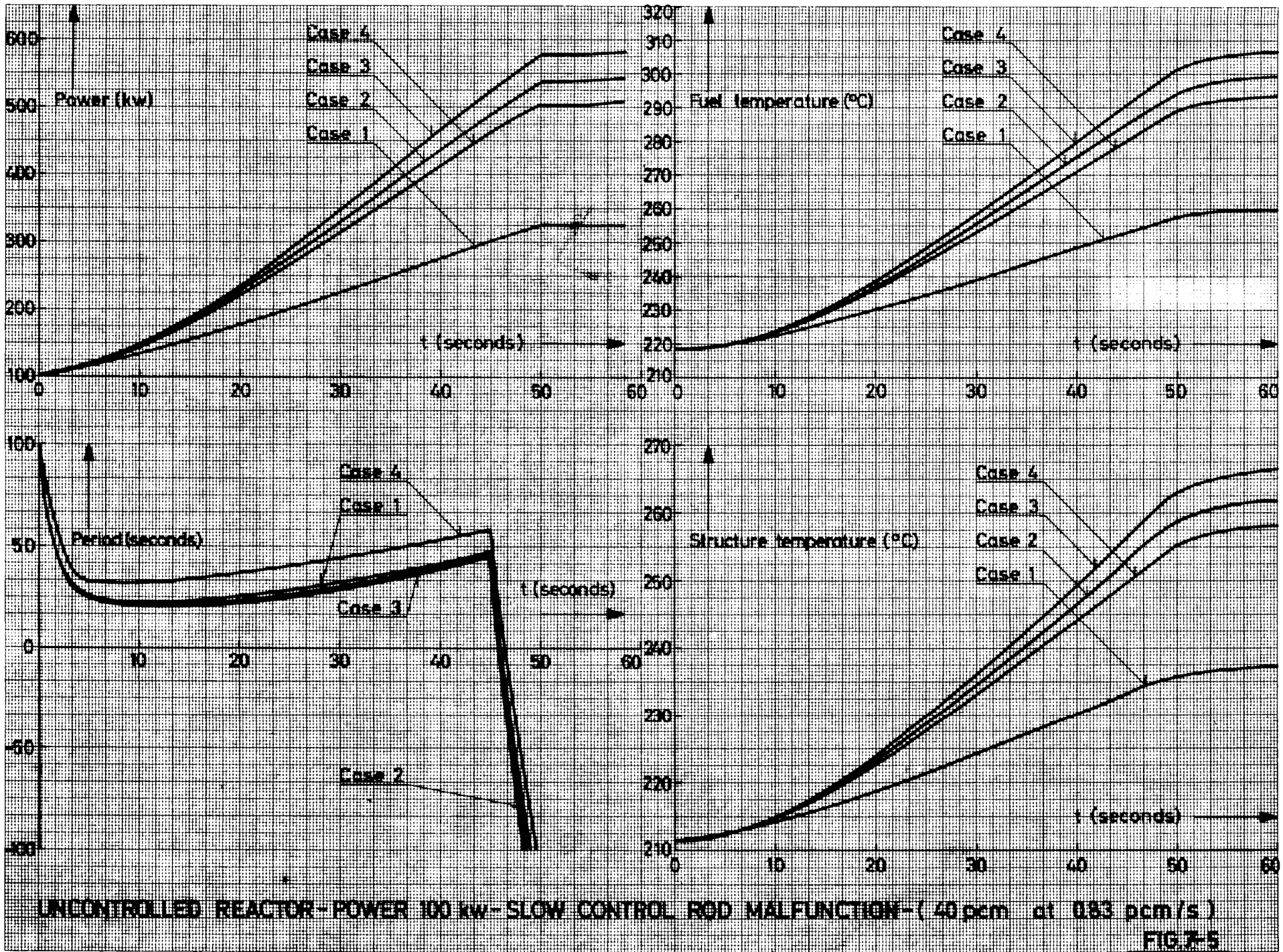
For each malfunction, and in each case, the following parameters have been plotted: power, period, fuel temperature, structure temperature. Results are presented in the figures from 7-1 to 7-6. Also the effect of a total loss of coolant flow occurring at 600 kW power has been investigated. The corresponding result is shown in figure 7-7.

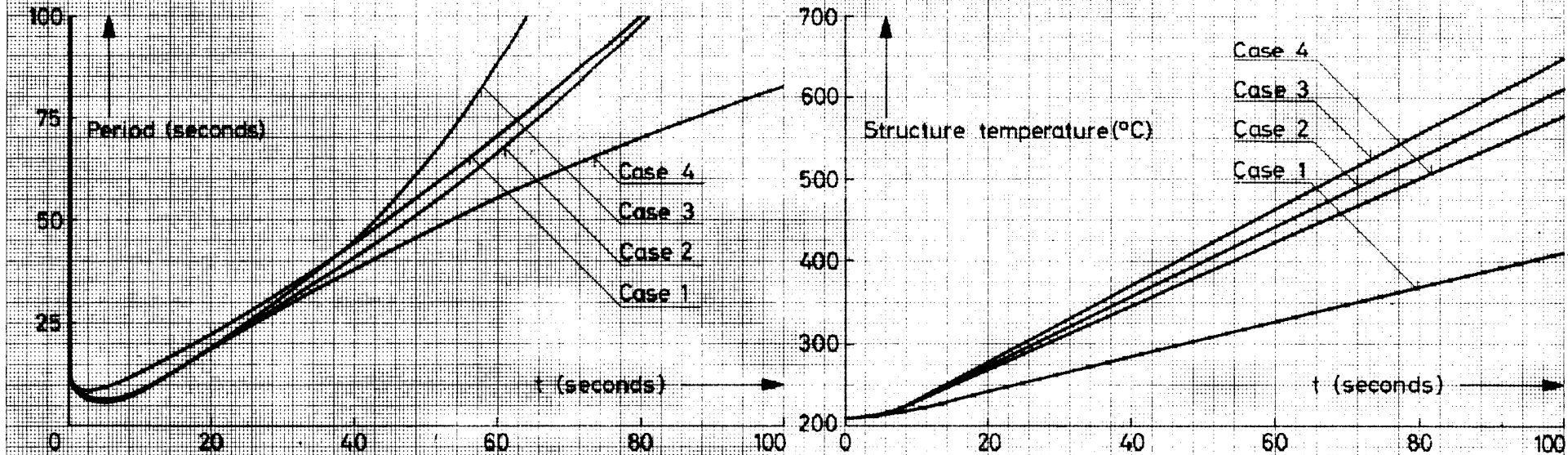
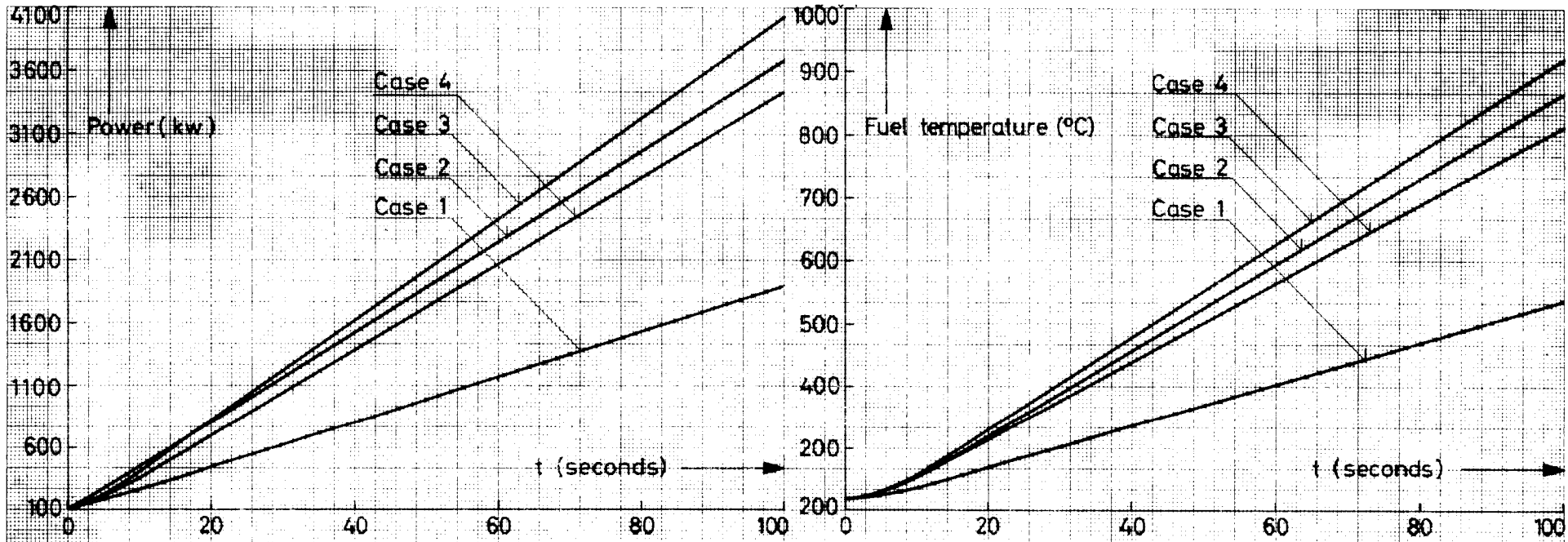












UNCONTROLLED REACTOR - POWER 100 kw - REGULATION ROD MALFUNCTION - (300 pcm at 3 pcm/s)

FIG. 7-5

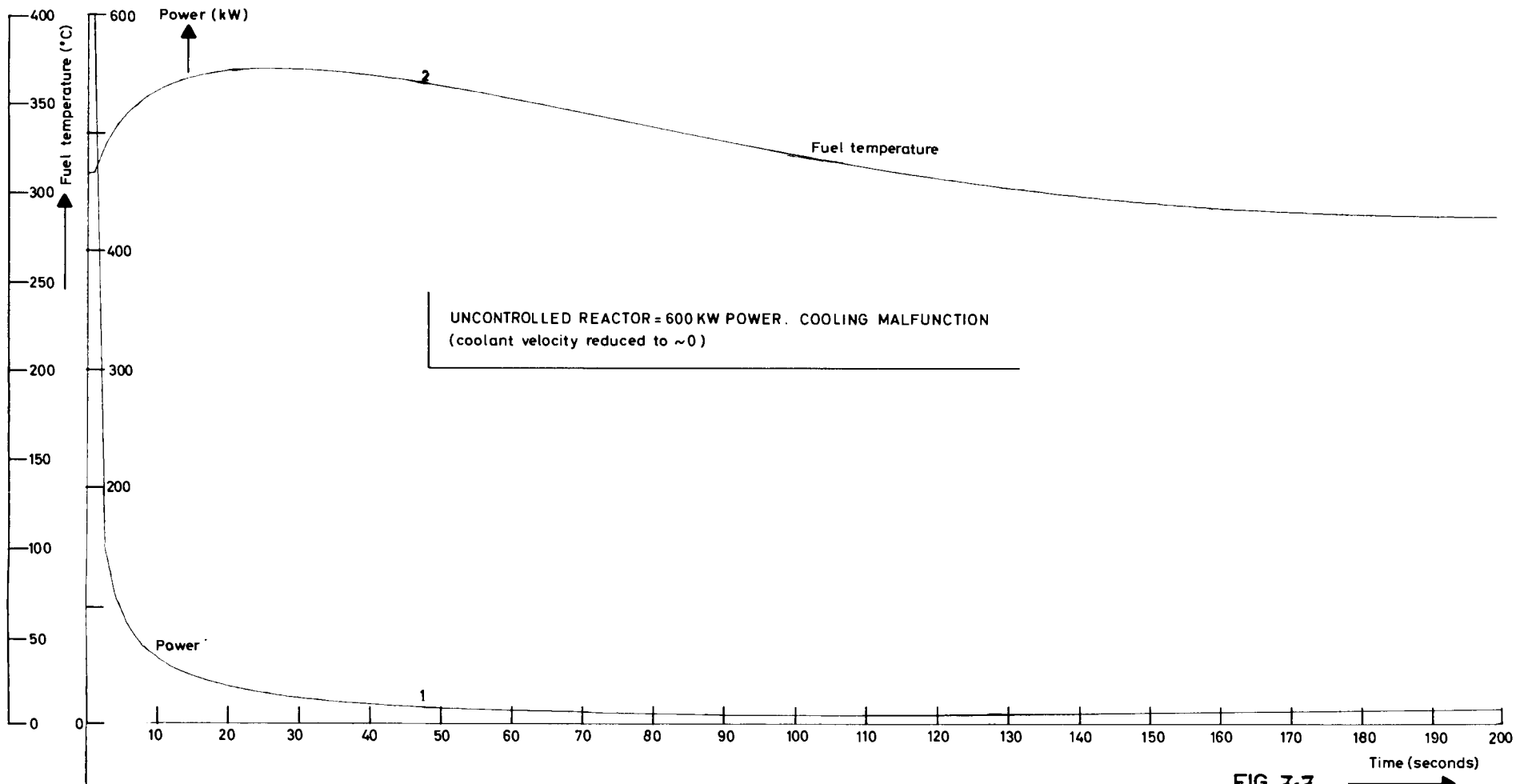


FIG 7-7

## Conclusion

As may be noted, this study has been performed using extensively only two programmes: the SAHYB-programme for simulation and the subroutine POLRT for finding the roots of polynomials. This method has proved to be powerful since it permitted - in a short time and without any difficulty - to answer most questions about the SORA dynamics and control, such as: reactor response to perturbations, start-up procedure, design of the fast control system, malfunctions, etc. Therefore, the initial choice of a digital computer for such a study seems retrospectively to be a good one.

Of interest also is the possibility of extending the simulation to the whole plant: the set of equations (6-4) may be completed with a heat exchanger description and safety circuits. In this manner, a complete logical start-up procedure should be defined.

However, the obtained results lie on the assumption of mean values equations as a reactor description. Although most important questions may be treated upon this basis, another study was started, based on a more accurate reactor kinetics description: the discrete time reactor description which consists of a set of recurrent equations. A comparison between the results obtained from this ultimate representation and the results presented here shows a posteriori the high degree of accuracy of the reactor description that we have used. This coincidence might be expected from the theoretical studies (Ref. 2 and 3).

Appendix 1 - Derivation of numerical values for a steady-state condition at power

Let us assume a pulsed steady state condition at power  $\bar{P}_0$ . We may neglect the contribution of the source-term  $S_0$ ; then we get the following set of equations for kinetics:

$$K = 0,229 + 8,80 \epsilon_m + 0,0176 e^{4140 \epsilon_m} = 1$$

$$\bar{w}_0 = \frac{K}{\beta v} \left( \sum_i \lambda_i \bar{C}_i + S_0 \right) \text{ with } K = 1$$

$$\frac{d\bar{C}_{i0}}{dt} = \beta_i v \bar{w}_0 - \lambda_i \bar{C}_{i0} = 0$$

$$\bar{P}_0 = \frac{\bar{w}_0}{C_F}$$

from which we derive  $\bar{w}_0 = C_F \bar{P}_0$  and successively:

$$\bar{C}_{10} = v \frac{\beta_1}{\lambda_1} \bar{w}_0$$

$$\bar{C}_{20} = v \frac{\beta_2}{\lambda_2} \bar{w}_0$$

⋮

etc.

⋮

$$\bar{C}_{60} = v \frac{\beta_6}{\lambda_6} \bar{w}_0$$

for the set of equations "thermal description", we get:

$$0 = \rho \bar{P}_0 - h_{FS} (\bar{T}_{fo} - \bar{T}_{go})$$

$$0 = h_{FS} (\bar{T}_{fo} - \bar{T}_{go}) - \frac{h_{sc}}{1 + \frac{h_{sc}}{2VC_c}} (\bar{T}_{go} - T_{c,in})$$

from which  $\bar{T}_{fo}$  and  $\bar{T}_{go}$  may be derived, while  $T_{c,out,0}$  and

$T_{c0}$  are calculated successively. Results are given here below:

$$\bar{C}_{10} = v \frac{\beta_1}{\lambda_1} C_F \bar{P}_o$$

$$\bar{C}_{20} = v \frac{\beta_2}{\lambda_2} C_F \bar{P}_o$$

$$\bar{C}_{30} = v \frac{\beta_3}{\lambda_3} C_F \bar{P}_o$$

$$\bar{C}_{40} = v \frac{\beta_4}{\lambda_4} C_F \bar{P}_o$$

$$\bar{C}_{50} = v \frac{\beta_5}{\lambda_5} C_F \bar{P}_o$$

$$\bar{C}_{60} = v \frac{\beta_6}{\lambda_6} C_F \bar{P}_o$$

$$\bar{T}_{fo} = T_{c,in} + \rho \bar{P}_o \left( \frac{1}{h_{FS}} + \frac{1}{h_{sc}} + \frac{L}{2VC_c} \right)$$

$$\bar{T}_{go} = T_{c,in} + \frac{\rho \bar{P}_o}{h_{sc}} \left( 1 + \frac{Lh_{sc}}{2VC_c} \right)$$

$$T_{c,out,o} = T_{c,in} + \rho \bar{P}_o \frac{L}{2VC_c}$$

$$T_{c0} = T_{c,in} + \rho \bar{P}_o \frac{L}{2VC_c}$$

Numerical values of these parameters at different power levels are given in the following table.

$\bar{P}_o$ (kW)	$\bar{c}_{10}$	$\bar{c}_{20}$	$\bar{c}_{30}$	$\bar{c}_{40}$	$\bar{c}_{50}$
100	$0,33383232 \times 10^{12}$	$0,45385316 \times 10^{13}$	$0,64990908 \times 10^{14}$	$0,80666532 \times 10^{14}$	$0,33245973 \times 10^{15}$
200	$0,66766471 \times 10^{12}$	$0,90770642 \times 10^{13}$	$0,12998183 \times 10^{15}$	$0,16133306 \times 10^{15}$	$0,66491972 \times 10^{15}$
300	$0,10014971 \times 10^{13}$	$0,13615596 \times 10^{14}$	$0,19497276 \times 10^{15}$	$0,24199960 \times 10^{15}$	$0,99737972 \times 10^{15}$
400	$0,13353290 \times 10^{13}$	$0,18154122 \times 10^{14}$	$0,25996368 \times 10^{15}$	$0,32266613 \times 10^{15}$	$0,13298397 \times 10^{16}$
500	$0,16691610 \times 10^{13}$	$0,22692661 \times 10^{14}$	$0,32495454 \times 10^{15}$	$0,40333259 \times 10^{15}$	$0,16622994 \times 10^{16}$
600	$0,20029941 \times 10^{13}$	$0,27231183 \times 10^{14}$	$0,38994545 \times 10^{15}$	$0,48399906 \times 10^{15}$	$0,19947594 \times 10^{16}$

Numerical values of parameters at different power levels.

SEE THE FOLLOWING PAGE

$C_{60}$	$\bar{T}_{fo} (^{\circ}C)$	$\bar{T}_{go} (^{\circ}C)$	$T_{c,out,o} (^{\circ}C)$	$T_{co} (^{\circ}C)$
$0,14895400 \times 10^{15}$	218,42065	211,45950	210,72224	205,36111
$0,29790779 \times 10^{15}$	236,84132	222,91902	221,44450	210,72224
$0,44686182 \times 10^{15}$	255,26199	234,37852	232,16675	216,08337
$0,59581585 \times 10^{15}$	273,68262	245,83806	242,88901	221,44450
$0,74476988 \times 10^{15}$	292,10327	257,29736	253,61125	226,80562
$0,89372391 \times 10^{15}$	310,52393	268,75708	264,33325	232,16673

Numerical values of parameters at different power levels (cont.)

Appendix 2 - Derivation of numerical values for a subcritical steady-state condition

We will calculate the numerical values for precursor concentrations and mean temperatures assuming that all of the control rods are removed. ( $\epsilon_d = 0$ ). The feedback reactivity may then be neglected ( $\epsilon_p = 0$ ), therefore  $\epsilon_m = 0$ , which gives the following value for the pulsed multiplication coefficient:

$$K = 0,2466$$

In such a steady state:

$$\frac{d\bar{C}_{10}}{dt} = \dots = \frac{d\bar{C}_{60}}{dt} = 0$$

which gives:

$$\begin{aligned} \bar{C}_{10} &= v \frac{\beta_1}{\lambda_1} \bar{w}_0 \\ &\vdots \\ &\vdots \\ \bar{C}_{60} &= v \frac{\beta_6}{\lambda_6} \bar{w}_0 \end{aligned}$$

In turns, these values are introduced into the equation:

$$\bar{w}_0 = \frac{K}{\beta v} \left( \sum_i \lambda_i \bar{C}_i + S_0 \right)$$

so that

$$\bar{w}_0 = \frac{K}{\beta v} \left( v\beta_1 \bar{w}_0 + \dots + v\beta_6 \bar{w}_0 + S_0 \right) = \frac{K}{\beta v} \left( \beta v \bar{w}_0 + S_0 \right).$$

The value for  $\bar{w}_0$  is derived from this last result:

$$\bar{w}_0 = \frac{K}{1-K} \cdot \frac{S_0}{\beta v}$$

and permits to calculate the precursor concentrations for the considered steady-state ( $K = 0,2466$ ). It is found:

$$\bar{C}_{i0} = \frac{1}{\lambda_i} \cdot \frac{\beta_i}{\beta} \cdot \frac{K}{1-K} \cdot S_0.$$

For such a steady-state, numerical values are:

$$\bar{C}_{10} = 2,202997 \cdot 10^4$$

$$\bar{C}_{20} = 2,995030 \cdot 10^5$$

$$\bar{C}_{30} = 4,2888294 \cdot 10^6$$

$$\bar{C}_{40} = 5,3232759 \cdot 10^6$$

$$\bar{C}_{50} = 2,19394090 \cdot 10^7$$

$$\bar{C}_{60} = 9,82964943 \cdot 10^6$$

and  $\bar{P}_0 = 6,599096 \cdot 10^{-6} \text{ kW}.$

Appendix 3 - Reactor period

The reactor period is defined as  $\frac{\bar{P}}{\frac{d\bar{P}}{dt}}$  or  $\frac{\bar{w}}{\frac{d\bar{w}}{dt}}$  ; this parameter

is of main interest during a start-up. We will outline the method which has been used to calculate this parameter. It consists of expressing the period in terms of the derivatives and functions which already appear in the set of equations (2-4) for the uncontrolled reactor. (Of course the derivation does not hold for the reactor submitted to control since other terms would appear in the final expression due to the control reactivity.)

$$\bar{w} = \frac{K}{\beta v} \sum_i \lambda_i \bar{C}_i$$

$$\frac{d\bar{w}}{dt} = \frac{1}{\beta v} \cdot \frac{dK}{dt} \cdot \sum_i \lambda_i \bar{C}_i + \frac{K}{\beta v} \sum_i \lambda_i \frac{d\bar{C}_i}{dt}$$

with

$$\frac{dK}{dt} = 8,80 \left( \frac{d\epsilon_d}{dt} + \frac{d\epsilon_{pf}}{dt} + \frac{d\epsilon_{pg}}{dt} \right) + 72,864 \left( \frac{d\epsilon_d}{dt} + \frac{d\epsilon_{pf}}{dt} + \frac{d\epsilon_{pg}}{dt} \right) e^{4,140\epsilon_m}$$

In our simulation the external reactivity  $\epsilon_d$  is always introduced under the form of a ramp function, so that the derivative  $(d\epsilon_d/dt)$  is the slope of this ramp and remains constant as long as this slope is not varied.

On the other hand  $\epsilon_{pf}$  and  $\epsilon_{pg}$  are related to the temperatures  $\bar{T}_f$  and  $\bar{T}_g$  so that we get for the derivative of K:

$$\frac{dK}{dt} = 8,80 \left( \frac{d\epsilon_d}{dt} + \alpha_f \frac{d\bar{T}_f}{dt} + \alpha_g \frac{d\bar{T}_g}{dt} \right) + 72,864 \left( \frac{d\epsilon_d}{dt} + \alpha_f \frac{d\bar{T}_f}{dt} + \alpha_g \frac{d\bar{T}_g}{dt} \right) e^{4,140\epsilon_m}$$

The reciprocal of the period is then expressed as:

$$\frac{1}{K} \cdot \frac{dK}{dt} + \frac{\sum_i \lambda_i \frac{d\bar{C}_i}{dt}}{\sum_i \lambda_i \cdot \bar{C}_i}$$

which is finally written under the form:

$$\frac{1}{K} \cdot \frac{dK}{dt} + \frac{K}{\beta v \overline{PC}_F} \cdot \sum_i \lambda_i \frac{d\overline{C}_i}{dt} .$$

We have used this last expression to calculate the reciprocal of the period, changing the  $\frac{d\epsilon_d}{dt}$  term as requested on account of the time interval under  $\frac{d\epsilon_d}{dt}$  calculation into the program.

Appendix 4 - Note on the simulation

Below is an example of how the simulation was performed. The subroutine DER describing the reactor [i.e. the complete set of equations (6-4)] is introduced into the main programme SAHYB. The case given simulates the response of the controlled reactor to a reactivity perturbation of 1 pcm, applied as a ramp function of 45 pcm/second slope. As may be noted, the subroutine DER calls in turn the subroutine DRAW, which enables the designer to get directly drawn the functions of interest. (In the present case, the power deviation was plotted as represented in Fig. 6-4-1 - curve 1).











ISI 1934  
ISI 1935

C  
C

RETURN  
EID

NOMENCLATURE

Symbol	Signification	Value	Units
$A_c$	coolant channel area per fuel element $A_c = 2\left(\sqrt{3} - \frac{\pi}{2}\right) r_o^2$	0.1814	cm <sup>2</sup>
$c_{bond}$	specific heat of bond	0.91	Wxs/g/°C
$C_{bond}$	heat capacity of bond per unit length $C_{bond} = 2\pi r_o \Delta r_{bond} \rho_{bond} c_{bond}$	0.066	Wxs/cm/°C
$c_c$	specific heat of coolant	0.91	Wxs/g/°C
$C_c$	heat capacity of coolant per unit length $C_c = A_c \rho_c c_c$	0.134	Wxs/cm/°C
$c_{clad}$	specific heat of clad	0.50	Wxs/g/°C
$C_{clad}$	heat capacity of clad per unit length $C_{clad} = 2\pi r_o \Delta r_{clad} \rho_{clad} c_{clad}$	0.550	Wxs/cm/°C
$c_f$	specific heat of fuel	0.19	Wxs/g/°C
$C_f$	heat capacity of fuel per unit length $C_f = \pi r_f^2 \rho_f c_f$	5.06	Wxs/cm/°C
$C_F$	conversion factor from fission rate to kW power $C_F = \frac{W}{P}$	$3.1 \times 10^{13}$	fission/(sec.kW)
$\bar{C}_i$	mean value of the i'th delayed neutron precursor concentration	function	without
G	amplifier gain (see fast control system)	12	
$h_f$	heat transfer coefficient from clad to coolant (Nu = 0,15.Pr <sup>0,34</sup> )	1.6	W/cm <sup>2</sup> /°C
$h_{Fs}$	heat transfer coefficient from fuel to mixed bond-clad	5.16	W/cm/°C
$h_{sc}$	heat transfer coefficient from mixed bond-clad to coolant	5.89	W/cm/°C
I	current through the motor	function	A

NOMENCLATURE cont.

Symbol	Signification	Value	Units
J	total inertia of the fast control device = (rotor moment of inertia + load of inertia)	$4.4 \times 10^{-3}$ $4.05 \times 10^{-3}$ $3.54 \times 10^{-4}$	$\text{kgm}^2$ $\text{kgm}^2$ $\text{kgm}^2$
k	back EMF coefficient for the motor	1.3	Volt/rad/s
$k_{\text{bond}}$	heat conductivity of bond	0.24	$\text{W/cm}^\circ\text{C}$
$k_{\text{c}}$	heat conductivity of coolant	0.24	$\text{W/cm}^\circ\text{C}$
$k_{\text{clad}}$	heat conductivity of clad	0.18	$\text{W/cm}^\circ\text{C}$
$k_{\text{f}}$	heat conductivity of fuel	0.24	$\text{W/cm}^\circ\text{C}$
$k_{\text{g}}$	heat conductivity of mixed bond-clad	0.20	$\text{W/cm}^\circ\text{C}$
	$k_{\text{g}} = \frac{\Delta r_{\text{bond}} + \Delta r_{\text{clad}}}{\frac{\Delta r_{\text{bond}}}{k_{\text{bond}}} + \frac{\Delta r_{\text{clad}}}{k_{\text{clad}}}}$		
K	pulsed multiplication coefficient $K = \frac{\text{precursor production during period}}{\text{precursor decay during period}}$	function	
l	self-inductance of the motor actuating the fast control rod	$2 \times 10^{-2}$	Henry
L	fuel rod height	24	cm
M	ratio of fissions in a pulse to the mean fission rate	function	second
n	number of fuel rods	116	-
p	conversion factor from kW into w	$10^3$	-
$\bar{P}$	mean power of the reactor (over one period)	function	kW
$\bar{P}_0$	nominal mean power	600	kW
q	average power generated in fuel per unit length = $\frac{p\bar{P}}{nL}$	function	$\text{W/cm}$
q''	average power generated in fuel per unit of area = $\frac{q}{2\pi r_f}$	function	$\text{W/cm}^2$

NOMENCLATURE cont.

Symbol	Signification	Value	Units
$q''$	average power generated in fuel per volume unit $= \frac{q}{\pi r_f^2}$	function	W/cm <sup>3</sup>
$r_o$	outer fuel element radius $r_o = r_f + \Delta r_{\text{bond}} + \Delta r_{\text{clad}}$	0.75	cm
$r_f$	fuel slug radius	0.70	cm
R	rotor resistance of the motor	6.7	ohm
$S_o$	neutron source	$10^7$	neutron/sec
T	period length of the pulsed reactor	$2 \times 10^{-2}$	second
$T_c$	mean coolant temperature (=temperature at half height core)	function	°C
$T_{c,\text{in}}$	inlet coolant temperature nominal value	function 200	°C °C
$T_{c,\text{out}}$	outlet coolant temperature	function	°C
$\bar{T}_f$	mean fuel temperature	function	°C
$\bar{T}_g$	mean bond-clad temperature	function	°C
$T_{\text{REF}}^*$	reference temperature for reactivity measurements	200	°C
$T_R$	reactor period ( $\bar{P}/d\bar{P}/dt$ )	function	second
V	voltage applied to the motor or at the input of the lead network or at the input of the whole system motor + tachometer	function	Volt
$U_c$	output of the lead network	function	Volt
U	coolant velocity in the channel nominal value	function 600	cm/s
$\bar{w}$	mean fission rate over a period	function	neutron/s
$\bar{w}_o$	nominal mean fission rate (corresponding to nominal mean power)	$1.86 \times 10^{16}$	neutron/s

NOMENCLATURE cont.

Symbol	Signification	Value	Units
$\alpha_f$	fuel temperature coefficient	-0.42	pcm/°C
$\alpha_g$	structure temperature coefficient	-0.80	pcm/°C
$\beta$	total delayed-neutron precursor production per fission neutron	$6.4 \times 10^{-3}$	-
$\beta_i$	i'th delayed neutron precursor production per fission neutron		
	$\beta_1$	$0.1668 \times 10^{-3}$	-
	$\beta_2$	$0.8184 \times 10^{-3}$	-
	$\beta_3$	$2.6066 \times 10^{-3}$	-
	$\beta_4$	$1.2024 \times 10^{-3}$	-
	$\beta_5$	$1.3615 \times 10^{-3}$	-
	$\beta_6$	$0.2444 \times 10^{-3}$	-
$\gamma$	conversion factor from the angular position of the fast control rod into pcm - $\gamma = \frac{10}{\pi}$	3.18	pcm/rad
$\Delta \bar{P}$	small power deviation from steady state resulting of a perturbation	function	kW
$\Delta \bar{P}_0$	small power demand from the nominal steady state 600 kW	function	kW
$\Delta r_{\text{bond}}$	bond thickness	0.02	cm
$\Delta r_{\text{clad}}$	clad thickness	0.03	cm
$\Delta \epsilon_d$	small external reactivity perturbation	function	pcm
$\Delta \epsilon_m$	small reactivity deviation from $\epsilon_{m0}$ $\left[ K(\epsilon_{m0}) = 1 \right]$	function	pcm

NOMENCLATURE cont.

Symbol	Signification	Value	Units
$\Delta\epsilon_p$	small feedback reactivity deviation from steady-state	function	pcm
	$\Delta\epsilon_p = + \begin{cases} \Delta\epsilon_{pf} \dots \text{from fuel} \\ \Delta\epsilon_{pg} \dots \text{from structure} \end{cases}$	function	pcm
$\epsilon_o$	average prompt reactivity between pulses (absolute value)	0.038	-
$\epsilon_c$	control reactivity from the fast control rod ( $\epsilon_c = \lambda\theta$ )	function	pcm
$\epsilon_d$	externally introduced reactivity	function	pcm
$\epsilon_m$	maximum prompt reactivity	function	pcm
$\epsilon_{mo}$	total reactivity at steady state = max prompt reactivity at steady state such as $K(\epsilon_{mo}) = 1$	91.1	pcm
$\epsilon_p$	feedback reactivity	function	pcm
$\epsilon_{pf}$	feedback reactivity from fuel	function	pcm
$\epsilon_{pg}$	feedback reactivity from structure	function	pcm
$\theta$	angular position of the fast control rod (starting from steady-state)	function	radian
$\lambda$	mean decay constant of delayed neutron precursor	0.08	(sec) <sup>-1</sup>
$\lambda_i$	decay constant of the i'th delayed neutron precursor		(sec) <sup>-1</sup>
	$\lambda_1$	3.8723	(sec) <sup>-1</sup>
	$\lambda_2$	1.3975	(sec) <sup>-1</sup>
	$\lambda_3$	0.31083	(sec) <sup>-1</sup>
	$\lambda_4$	0.11552	(sec) <sup>-1</sup>
	$\lambda_5$	0.031738	(sec) <sup>-1</sup>
	$\lambda_6$	0.012716	(sec) <sup>-1</sup>

NOMENCLATURE cont.

Symbol	Signification	Value	Units
$\eta$	gain of the tachometer dynamo	0.5	Volt/ (rad/sec)
$\nu$	total number of neutrons (prompt and delayed) produced per fission	2.5	-
$\rho$	conversion factor from mean power $\bar{P}$ generated in the reactor into average power $q$ generated in fuel per unit length $= \frac{p}{nL}$	0.359	(cm) <sup>-1</sup>
$\rho_{\text{bond}}$	specific mass of bond	0.81	g/cm <sup>3</sup>
$\rho_c$	specific mass of coolant	0.81	g/cm <sup>3</sup>
$\rho_{\text{clad}}$	specific mass of clad	7.92	g/cm <sup>3</sup>
$\rho_f$	specific mass of fuel	17.3	g/cm <sup>3</sup>
$\tau$	electromechanical time constant of the fast control system (motor + control rod)	$18.5 \times 10^{-3}$	second
$\tau'$	electrical time constant of the motor ( $\tau' = \frac{1}{R}$ )	$3 \times 10^{-3}$	second
$\omega_1$	zero of the compensation network introduced in the fast control system	$10^2$	rad/sec
$\omega_2$	pole of the compensation network introduced in the fast control system	$5 \times 10^2$	rad/sec

LITERATURE

- 1.) I.L.BONDARENKO and Yu. Ya. STAVISKII  
Atomnaya Energiya, 7, 417 (1959)  
Reactor Science and Technology, 14, 55 (1961)
- 2.) G.BLAESSER, R.MISENTA and V.RAIEVSKI  
"The kinetic theory of a fast reactor periodically pulsed by reactivity variations"  
EUR 493 e -Euratom - Ispra - Italy (1965)
- 3.) J.A.LARRIMORE  
"Physics of a periodically pulsed Reactors and Boosters: Steady-state conditions, Power-pulse characteristics, and kinetics"  
Nuclear Science and Engineering: 29, 87-110 (1967)
- 4.) J.A.LARRIMORE, R.HAAS, K.GIEGERICH, V.RAIEVSKI, W.KLEY  
"SORA - paper presented at American Nuclear Society National Topical Meeting on fast burst reactors - Jan. 28-30, 1969 - Albuquerque - New Mexico.
- 5.) F.STORRER  
" Temperature response to power, inlet coolant temperature and flow transient in solid fuel reactors"  
June 1959 - ADPA 130  
Atomic Power Development Associates, Inc.
- 6.) V.RAIEVSKI et al.  
" The pulsed fast reactor as a source for pulsed neutron experiments"  
Proc. IAEA Symposium on pulsed neutron research - Karlsruhe 1965  
Vol. II, 553.
- 7.) J.A.LARRIMORE, R.HAAS, K.GIEGERICH, V.RAIEVSKI and W.KLEY  
" The SORA Reactor; Design Status Report"  
AEC - ENEA - Seminar on intense Neutron Sources - Santa Fé (1966)

- 8.) J.RANGLES  
" Feedback due to elastic waves and Doppler coefficient during the excursions of the Pulsed Fast reactor"  
J. Nucl. Energy - A/B, 20,1 (1966)
- 9.) H.D'HOOP and R.MONTEROSSO  
" SAHYB 2 - A programme for the solution of differential equations using an analogue - oriented language"  
EUR 3622 e - Euratom - Ispra - Italy
- 10.) R.ARHAN, F.SCIUTO  
" SORA Zero power transfer function - Steady state and pulsed operation"  
Internal Report ISPRA 700
- 11.) Subroutine POLRT  
Available at CETIS  
EURATOM- C.C.R. - ISPRA - Italy
- 12.) G. BLAESSER and J.A.LARRIMORE  
" Discrete kinetics for periodically pulsed fast reactor"  
Nucl. Sci. Eng. (in press)
- 13.) R.ARHAN, P.BARBASTE, D.COCHET, F.SCIUTO  
" Eleven progress reports: SORA Control and Simulation Studies from 15.10.67 / to 30.9.68.



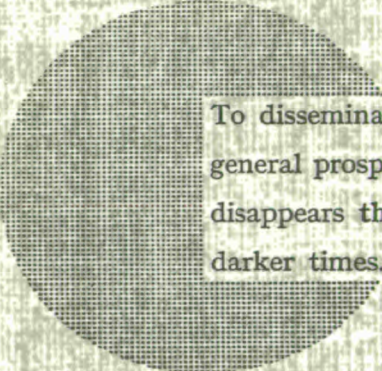
### NOTICE TO THE READER

All Euratom reports are announced, as and when they are issued, in the monthly periodical **EURO ABSTRACTS**, edited by the Center for Information and Documentation (CID). For subscription (1 year : US \$ 16.40, £ 6.17) or free specimen copies please write to :

**Handelsblatt GmbH**  
**"Euro Abstracts"**  
**Postfach 1102**  
**D-4 Düsseldorf (Germany)**

or

**Office de vente des publications officielles**  
**des Communautés européennes**  
**37, rue Glesener**  
**Luxembourg**



To disseminate knowledge is to disseminate prosperity — I mean general prosperity and not individual riches — and with prosperity disappears the greater part of the evil which is our heritage from darker times.

Alfred Nobel

## SALES OFFICES

All Euratom reports are on sale at the offices listed below, at the prices given on the back of the front cover (when ordering, specify clearly the EUR number and the title of the report, which are shown on the front cover).

### OFFICE DE VENTE DES PUBLICATIONS OFFICIELLES DES COMMUNAUTES EUROPEENNES

37, rue Glesener, Luxembourg (Compte chèque postal N° 191-90)

#### BELGIQUE — BELGIË

MONITEUR BELGE  
40-42, rue de Louvain - Bruxelles  
BELGISCH STAATSBLAD  
Leuvenseweg 40-42 - Brussel

#### LUXEMBOURG

OFFICE DE VENTE DES  
PUBLICATIONS OFFICIELLES DES  
COMMUNAUTES EUROPEENNES  
37, rue Glesener - Luxembourg

#### DEUTSCHLAND

BUNDESANZEIGER  
Postfach - Köln 1

#### NEDERLAND

STAATSDRUKKERIJ  
Christoffel Plantijnstraat - Den Haag

#### FRANCE

SERVICE DE VENTE EN FRANCE  
DES PUBLICATIONS DES  
COMMUNAUTES EUROPEENNES  
26, rue Desaix - Paris 15°

#### ITALIA

LIBRERIA DELLO STATO  
Piazza G. Verdi, 10 - Roma

#### UNITED KINGDOM

H. M. STATIONERY OFFICE  
P. O. Box 569 - London S.E.1

EURATOM — C.I.D.  
29, rue Aldringer  
L u x e m b o u r g

CDNA04408ENC